

See discussions, stats, and author profiles for this publication at: <https://www.researchgate.net/publication/262773483>

Biomimetic Synthesis of Shaped and Chiral Silica Entities Templated by Organic Objective Materials

ARTICLE *in* CHEMISTRY - A EUROPEAN JOURNAL · JUNE 2014

Impact Factor: 5.73 · DOI: 10.1002/chem.201400387

CITATIONS

6

READS

358

3 AUTHORS, INCLUDING:

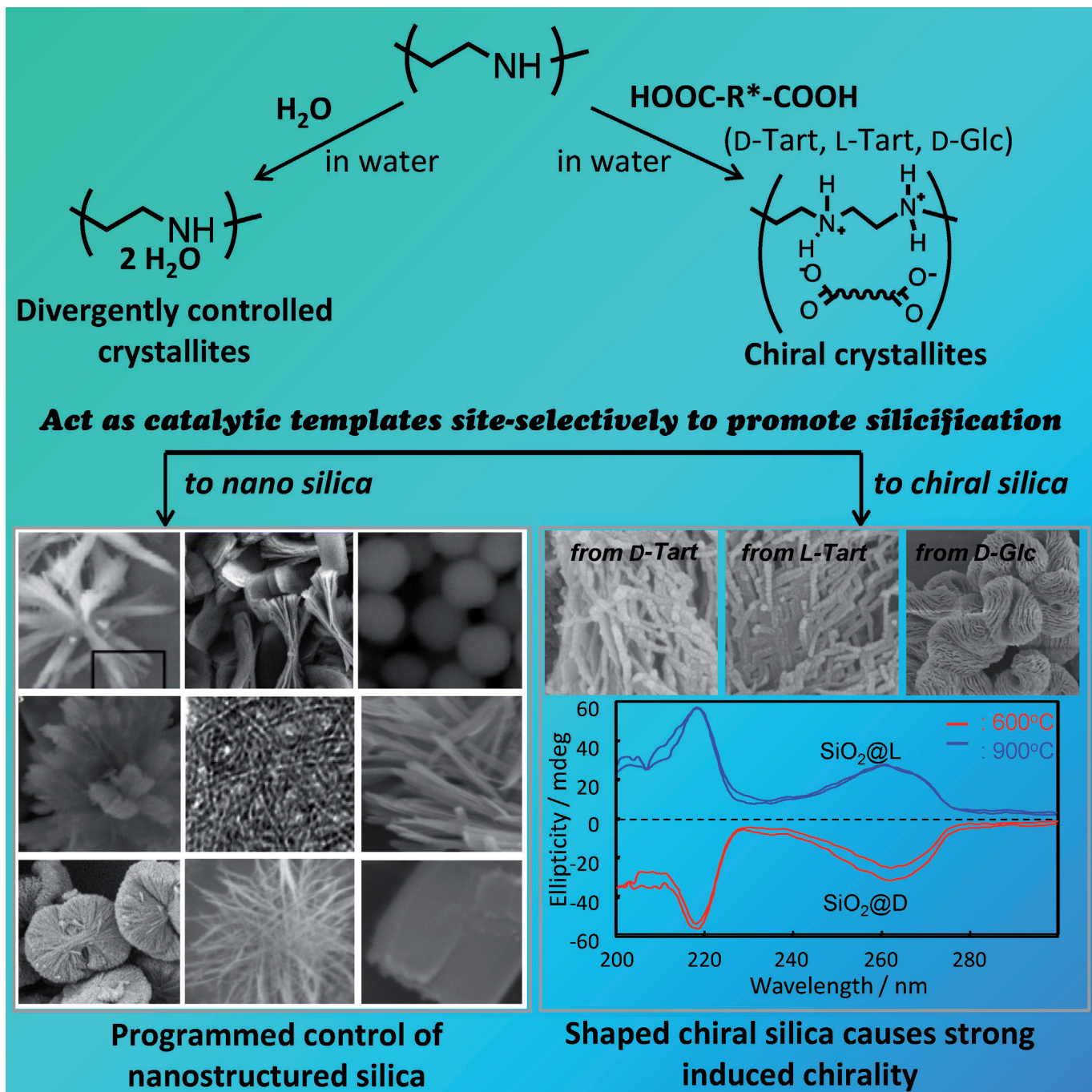


ren-hua Jin

Kanagawa University

70 PUBLICATIONS 1,200 CITATIONS

SEE PROFILE

Self-Assembly**Biomimetic Synthesis of Shaped and Chiral Silica Entities Tempered by Organic Objective Materials**Ren-Hua Jin,* Dong-Dong Yao, and Rumi (Tamoto) Levi^[a]

Abstract: Organic molecules with accompanying self-organization have been a great subject in chemistry, material science and nanotechnology in the past two decades. One of the most important roles of organized organic molecules is the capability of templating complexly structured inorganic materials. The focus of this Minireview is on nanostructured silica with divergent morphologies and/or integrated chirality

directed by organic templates of self-assembled polyamine/polypeptides/block copolymers, chiral organogels, self-organized chiral amphiphiles and chiral crystalline complexes, etc., by biomimetic silicification and conventional sol-gel reaction. Among them, biosilica (diatoms and sponges)-inspired biomimetic silicifications are particularly highlighted.

Introduction

In nature, there are many examples of exceptionally strong building materials formed by organic-inorganic assemblies. This organization widely exists in the skeletons of animals or plants, and plays a key role in expressing the biological functions. These materials often show the complex hierarchical organization from the nanometric to macroscopic scales.^[1,2] Bio-mineralization promoted by organic templates often produces organized materials with hierarchical structures composed of organic and inorganic components. In recent years, much effort has been directed towards developing organic-inorganic hybrid materials to mimic and understand the complex structure-property relationship of their natural counterparts. Biomimetic mineralization from synthesized organic templates offers the possibility to engineer complex architectures starting from nanometric regime ("bottom-up" fabrication). One such method is inspired from self-assembled organic systems, which can form various structures that can be used as templates for inorganic nanomaterial formation. Particularly, there have been many reports of silica-based materials with controllable shapes, porosity and chirality generated from organic templates because silica-based materials are important for a wide range of technological applications, such as catalysts, polymeric fillers, coatings, chemical and biological separations, sensors, photonic and electronic devices, bioencapsulation, enzyme immobilization, bioimaging, drug delivery, and so on.^[3]

It is widely known that silica is a very abundant natural material. Long before the beginning human, living things composed of silica bodies, such as diatoms and sponges, worked unremittingly for balancing the atmospheric environment of the Earth through billions of years of evolutionary steps. Diatoms and sponges living in fresh water or marine environment consume carbon dioxide by photosynthesis and produce lipid compounds. This is most unique to diatoms and sponges and starts the food chain for fish and shellfish living in aqua. Another global-scale event is that marine organisms, diatoms and sponges produce more than six gigatons of silicon each year to build their silica cell wall or skeletons.^[4] Surprisingly, in such silicon production, the organisms design exquisite hierarchical structures and multiple morphologies with precise

nanoscale control in their silica skeleton.^[5,6] So we think of the occurrence of silica biominerization in diatoms and sponges as an eternal text and source of inspiration for the design and synthesis of silica-based nano/microscale materials, including chiral silica and related metal oxides. In fact, the attraction of humans to diatoms as well sponges due to their aesthetic and geometrically precise symmetric patterns and special shapes goes back to the early nineteenth century during which time there was emerging improvements in microscopy resolution.^[7] However, the recognition of the aesthetic structures of diatoms and sponges by chemists is a recent event of the past 15 years. The pioneering work performed independently by the Sumper and Morse groups has shed new light on understanding and mimicking diatoms and sponges. The Sumper group extracted organic matrices from the solution of hydrolyzed cell wall of diatom silica skeleton and revealed that the organic matrices are short-chain length peptides (silaffins) and/or long-chain polyamines with different unit structures.^[8] They further confirmed that these isolated organic matrices promote the silica deposition *in vitro* under very mild conditions.^[8c,d] Particularly, different species of diatoms have specific long-chain polyamines, which play an important role in polymerization of silicic acid. In contrast to Sumper's approach, the Morse group^[9] have paid attention to spicules of the sponge *Tethya aurantia*.^[9a] They isolated the filament cores from the hydrolyzing silica shell and found that the filaments consist of silica proteins (silicateins). Interestingly, the filament fibrils possessing the amino acids His and Ser in the protein sequences play a decisive role in promoting silicification on their surface without any additional catalysts.^[9b] They showed that hydrogen bonds formed between the hydroxyl on the Ser residue and the imidazole on His worked as the active site for hydrolytic condensation of alkoxy silanes.

For the design of organic-inorganic materials, the main aim is not to simply emulate particular biological architectures and systems, but also to elucidate the mechanistic intricacy involved in these processes, and use such knowledge for the preparation of new synthetic materials and devices.^[10,11] A series of achievements from the Sumper laboratory working on diatoms and the Morse laboratory studying sponges has imparted great information and changed the research status of traditional silica mineralization based on pH controlled sol-gel chemistry. The finding that long-chain polyamines/peptides and solid fibrils of proteins play a dual role as template and catalyst in silica deposition under ambient conditions and nearly neutral aqueous media has stimulated chemists to

[a] Prof. R.-H. Jin, Dr. D.-D. Yao, Dr. R. Levi

Department of Material and Life Chemistry, Kanagawa University
3-2-7 Rokkakubashi, Yokohama 221-8686 (Japan)
E-mail: rhjin@kanagawa-u.ac.jp

Table 1. Comparison of different strategies for synthesis of structured silica.

Strategies	Advantages	Drawbacks
biomimetic silicification	templates can act as catalysts to control the silicification temporally and spatially mild reaction conditions (water as solvent, RT and atmospheric pressure, low cost and environmentally friendly) diverse and controlled structures	design and formation of templates with special chemical composition
conventional template sol-gel synthesis	relatively extensive template selection versatile approach for structure control by gelation around templates precisely controlled mesopore materials	additional base or acid as catalyst harsh reaction conditions (organic solvents, high temperature and/or pressure, long reaction time) easy to produce nontemplated silica multiple steps for preparation

design sophisticated molecular models to direct structured silica through such biomimetic approaches. In particular, templating by amine-bearing polymers or surfactants for silicification is one of the successful biomimetic approaches for fabricating shaped silica hybrids and hollow silica under mild and environmentally friendly conditions. The amine-bearing polymers, such as polyamines and polypeptides, which are capable of efficiently promoting hydrolytic condensation of the silica source at ambient temperature and neutral pH, usually form various polymeric aggregates in different conditions. Furthermore, the shape of the silica hybrids and hollow silica is strongly dependent on the template shape, and the composition of the hybrids can be adjusted by different Si/N mole ratios and reaction times. So, much attention has been paid to the preparation of various and novel polymer templates among researchers in the last decade.

This is also an attractive subject in silica-related materials; that is, chiral silica with imparting chirality onto silica skeletons by chiral transfer from chiral organic templates. However, early studies on chiral silica construction are not based on the concept of biomimetic silicification. Chiral aggregates only act as chiral templates but do not work as catalysts. Therefore, silica deposition on chiral templates often needs additional catalysts, such as HCl, or basic compounds. This is one drawback of producing silica sol independently of chiral templates, thus reducing the site-selectivity of silica deposition on chiral templates although a limited part of helical silica images (TEM and SEM) is often perfect.

In order to distinguish the differences between biomimetic silicification and conventional templated sol-gel reaction, we compare briefly their advantages and drawbacks in Table 1.

This review focuses on recent progress in silica materials, with respect to shape and chirality control, based mainly on the biosilica-inspired approach employing specially designed templates. Because many chiral silicas are not completely constructed through the biomimetic silicification route, we also highlight the conventionally templated chiral silica for an overview of the potential of chiral silica, which is one of the most interesting topics of bioinspired-silica materials.

Ren-Hua Jin graduated from Jilin University (Changchun, China) in 1982 and completed his PhD study in the synthesis and application of chiral ligand polymers with chiral discrimination of racemic amino acids at Nankai University (Tianjin, China) in 1987. After that, he joined Beijing University of Chemical Technology as an assistant professor for a period of 2 years and transferred to the University of Tokyo as a postdoctoral fellow. He worked at Miyazaki University as an associate professor from 1994 to 1997. Then, he worked in Kawamura Institute of Chemical Research as a leader for 14 years and moved to Kanagawa University as a full professor in April 2012. His current research interests lie in the architecture of water-soluble/amphiphilic polymers, design of ceramic nanomaterials with shape- and/or chirality-control, and their applications in catalysis, energy-conversion, wettability control, sensing, etc.



Dong-Dong Yao completed his Bachelor's degree in Chemistry at Xi'an University, China. Then he received his Master's degree in 2010 from Shaanxi Normal University, China. He obtained his PhD from Institute of Chemistry, The Chinese Academy of Sciences (ICCAS) in 2013 under the supervision of Prof. Yong-Ming Chen, working on the preparation of shaped functional nano-objects based on microphase separation of diblock copolymers in bulk. He joined the group of Prof. Ren-Hua Jin at Kanagawa University as a postdoctoral researcher in August 2013. His current research interests mainly focus on synthesis and self-assembly of polyamine-bearing polymers, and their potential applications.



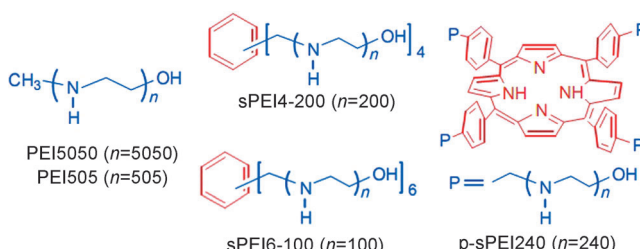
Rumi Levi (Tamoto) graduated from Kumamoto University and received her Masters degree in Chemistry in 2007 from the Kumamoto University, Japan. She then moved to the University of Bordeaux 1, France, where she worked on self-assembled chiral structures using achiral cationic amphiphiles in the presence of chiral counter-anion, and completed her PhD thesis in physical chemistry in 2011, at the laboratory CBMN with Dr. Reiko Oda. Consequently, she worked at CBMN on organic-inorganic chiral hybrid materials until 2012. In September 2013, she moved to Yokohama, Japan, where she works mainly on quaternized cationic polymers and its self-assembled systems under the supervision of Prof. Ren-Hua Jin in Kanagawa University.



Polyamine-Based Materials as Templates and Catalysts

Polyamine-based aggregates

Polyethyleneimine (PEI)-based aggregates: PEI, possessing only secondary amine units in its backbone, is particularly interesting due to its crystalline features in aqueous media. The free-base form of PEI as a crystalline polymer is capable of crystallizing either as PEI alone or through a PEI/H₂O two-component association. The latter is based on hydrogen-bond formation between the ethyleneimine unit ($-\text{CH}_2\text{CH}_2\text{NH}-$) and H₂O as different ratios of ($-\text{CH}_2\text{CH}_2\text{NH}-$)/H₂O (0.5) can significantly alter the crystalline structures. Such water-containing crystalline powders are insoluble in ambient water or general organic solvents, with the exception of methanol. This characteristic crystalline state can appear in nanoscale self-assembly to produce shaped crystalline aggregates with high density of amine residues in their surface. Such aggregates are ideal candidates for catalytic templates for biomimetic silicification because they are not only similar to the long-chain polyamines isolated in diatoms but also resemble the filaments of silicateins seen in sponge spicules. With such a concept, we used the aggregates as a catalyst, template and scaffold to direct the formation of silica with controllable composition and various complex spatial structures from hydrolytic condensation of alkoxy-silanes under mild conditions. We have established a programming methodology to fabricate silica hybrid materials with multiple morphologies. Linear and star PEIs (LPEI and sPEI Scheme 1) programmably self-organize into ordered aggre-



Scheme 1. Different PEI molecular structures.^[12]

gates with the morphologies of nanowires, fibrous bundles, nanofiber-based networks, flowers, plates and nanograss, etc. The shapes can be affected by various factors, such as polymer architecture, PEI concentration, acidic or metal-ion additives, temperature, etc.^[12]

Polymer architecture: Silica morphology could be adjusted by changing topological architectures of PEI.^[12a,b,o] We obtained silica with bundlelike, leaflike, fibrous, and aster-like shapes by using PEI with three topological structures of linear type and star with two different cores (LPEI5050, sPEI₆-100 and *p*-sPEI₄-240), respectively (Figure 1). As shown in Figure 1 a and b, silicification templated by using LPEI5050 aggregates with concentrations of 2 and 0.25 wt% exhibited the expanded bundle and leaf morphologies, respectively. In contrast, a six-

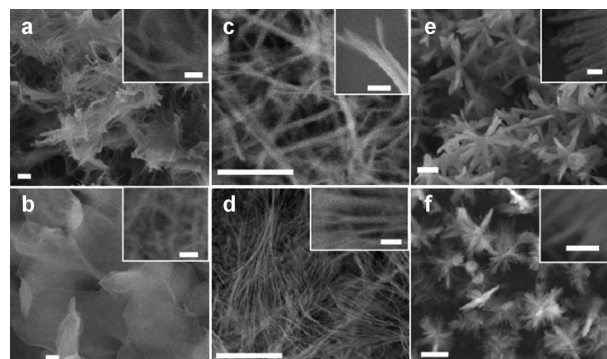


Figure 1. Shaping silicas by designing linear PEI backbones into star architectures. SEM images of PEI@silicas prepared by using PEI5050 with concentrations of: a) 2.0 wt%, and b) 0.25 wt%; using sPEI₆-100 with concentrations of: c) 2.0 wt%, and d) 0.25 wt%; and *p*-sPEI₄-240 with concentrations of: e) 2.0 wt%, and f) 0.25 wt%. Scale bars are 2 μm and 100 nm for insets.^[12o]

armed star PEI with a small benzene core (sPEI₆-100) directed the formation of silica with a fibrous framework and looser nanofiber bundles (Figure 1 c and d). In addition, the silica with multi-armed aster-like shape were achieved by using a star PEI with porphyrin core (*p*-sPEI₄-240; Figure 1 e and f).

PEI concentration: One of the effective methods for regulating shapes of PEI aggregates was to change the concentration of PEI in aqueous media. The effect of concentration of PEI on silica hybrid morphologies was studied by performing silicification reaction on the aggregates from LPEI500 and sPEI₄-200 with concentrations from 5.0 to 0.1 wt% using tetramethoxysilane (TMOS) as silica precursor at room temperature (Figure 2 and Figure 3). It was found that the morphologies and struc-

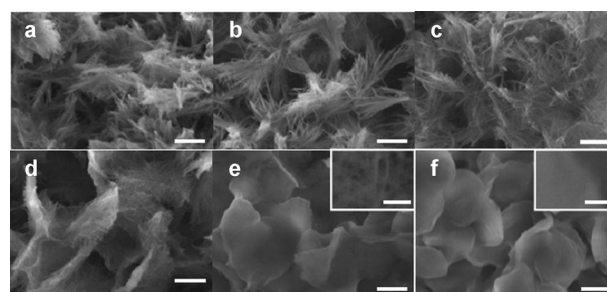


Figure 2. Morphological dependence of PEI@silica on the concentration of PEI505. SEM images of PEI@silica synthesized with PEI505 aggregates with concentrations of: a) 5, b) 3, c) 2, d) 0.5, e) 0.25, and f) 0.1 wt%. Scale bars are 5 μm and 500 nm for insets in e and f.^[12o]

tures of the silica hybrids were strongly dependent upon the concentration of PEI. At higher concentrations from 5 to 2 wt%, the silica appeared as fiber-based bundles with a size of several micrometers; these changed to curved leaf-like film composed of interwoven nanofibers as the concentration of PEI decreased to 0.5 wt%. When PEI concentration decreased to 0.1 wt%, a thicker silica film showed a smooth surface without fiber structure, which might arise from fiber-fiber linking and integration.^[12c,d,o]

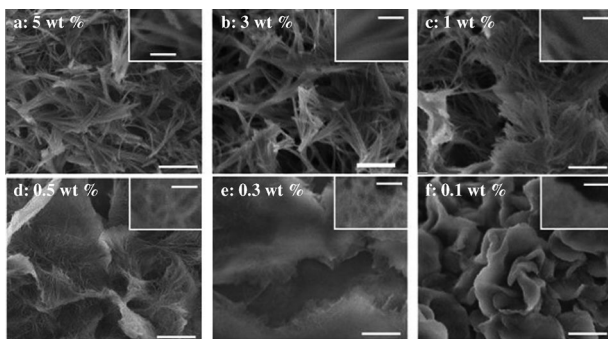


Figure 3. SEM images of silicas mediated from various concentrations of sPEI4-200 in neat water as medium. Silicas in panels a–f were mediated from polymer concentrations of 5, 3, 2, 1, 0.5, 0.3 and 0.1%, respectively. Scale bars are 5 μ m and 500 nm for insets.^[12d] Copyright © 2006, American Chemical Society.

Acidic additive: Acidic conditions are another important factor in PEI-based silica deposition for control of silica structure due to proton transfer interaction between the EI unit and the acid. We prepared a series of crystalline precipitates of LPEI associated with proton-donating compounds, such as tris(hydroxymethyl) aminomethane-HCl (Tris-HCl), D-tartaric acid and L-amino acids for silica-directing formation.^[12e,f] It was found that both concentration and category of acidic additives affected the morphologies of precipitates, and the self-organized precipitates produced precisely directed bent nanosheets of silica-LPEI hybrids (Figures 4 and 5).

Metal-ion additive: Metal ions can also efficiently regulate the morphology of PEI aggregates by strong coordination interactions between the EI unit and metal cations.^[12g] PEI aggregates under the mediation of metal ions were fabricated by slow cooling of hot aqueous solutions of PEI containing metal

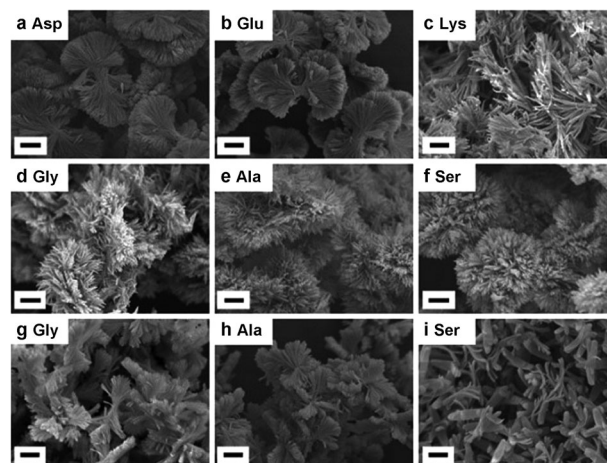


Figure 5. Hierarchical silica transcribed from precipitates which were formed in LPEI/L-amino acid aqueous solutions. a) L-Aspartic acid, b) L-glutamic acid, c) L-lysine, d, g) glycine, e, h) L-alanine, f, i) L-serine. Concentrations of amino acids in the solutions were 200 (a–f) or 1000 mM (g–i). In all solutions, concentrations of LPEI were fixed to 1000 mM for EI units. Scale bars: 2.00 μ m.^[12f] Copyright © 2010, Springer Science+Business Media B. V.

cations with different valence states (Na^+ , Cu^{2+} , Al^{3+} , etc.). The silicification was subsequently conducted by mixing the aggregates with TMOS at room temperature. Finally, silica with bulky, turbine-like and urchin-like shapes were produced by mediation of Na^+ , Cu^{2+} and Al^{3+} , respectively (Figure 6).

Such nanostructured silicas can be used as matrices for loading metallic or metal oxide nanoparticles, which act as catalysts^[12l] or luminescent materials.^[12m] In addition, the nanostructured silica can be reduced to the corresponding nanostructured silicon.^[12n] which can be applied as anode material in lithium-ion batteries.

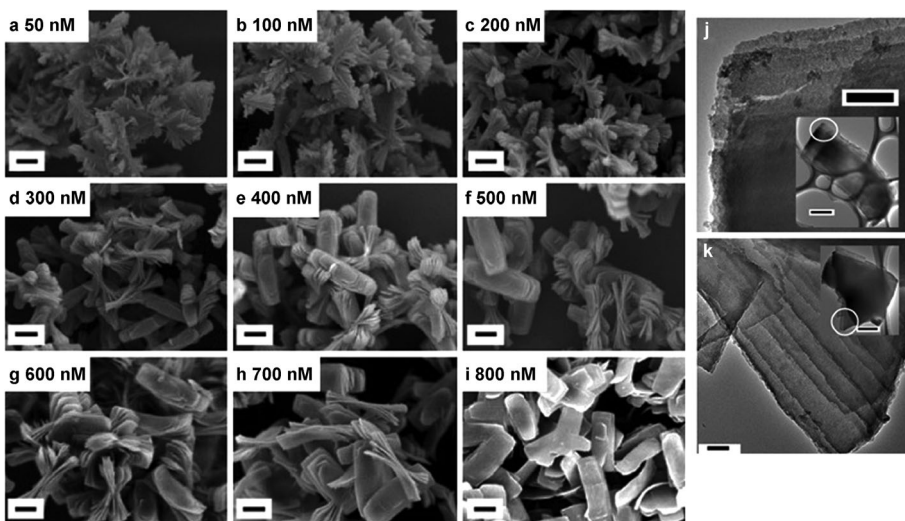


Figure 4. SEM and TEM images of hierarchical silica transcribed from precipitates which were formed in LPEI/Tris-HCl aqueous solutions. In all solutions, the concentration of LPEI was fixed to 1000 mM for EI units. For SEM images, the concentrations of Tris-HCl were: a) 50, b) 100, c) 200, d) 300, e) 400, f) 500, g) 600, h) 700, and i) 800 mM; scale bars: 2.0 μ m. TEM images of bent nanosheet samples: j) close view (scale bar: 200 nm) of the circled part of one piece of nanosheet (inset, scale bar: 1 μ m) and; k) close view (scale bar: 100 nm) of circled part of inset (inset, scale bar: 1 μ m).^[12e] Copyright © 2010, Springer Science+Business Media B. V.

Although the silica appearances mediated by crystalline LPEI templates are different in micro-scale, the silica structures can be divided into two basic types: one is silica nanofiber-based assemblies towards two- or three-dimensions, and the other is silica nanoribbon (or nanosheet)-based assemblies. LPEI crystalline aggregates which grow rapidly can produce fibrous silica structures, while the slowly formed LPEI crystalline aggregates tend to produce nanosheet silica. For example, the aggregates obtained by rapid cooling with addition of ice to a hot aqueous solution of LPEI, favor nanofiber-based silica structures.^[12l] In contrast, aggregates obtained by slow crystallization with the addition of definite amounts of proton donor, such as Tris-HCl,

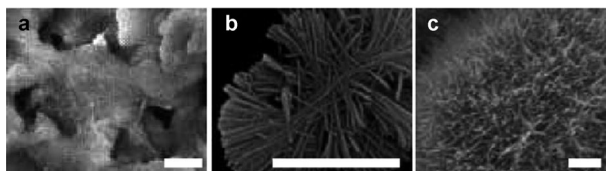


Figure 6. SEM images of shaped silicas from self-assembled PEI aggregates mediated by metal ions: a) Na^+ , b) Cu^{2+} , and c) Al^{3+} , with molar ratio of PEI to metal ions of 20:1. Scale bars: 2 μm .^[12g] Copyright © 2007, WILEY-VCH Verlag GmbH & Co. KGaA, Weinheim.

to a hot aqueous solution of LPEI direct nanosheet-based silica.^[12e]

Aggregates formed on arbitrary substrates: We have successfully constructed silica nanograss, nanowire and other complex nanotextured silica film on substances (plastics, glasses, or metals) with arbitrary shapes (films, plates, tubes, or rods; Figure 7). Firstly, the nanostructured LPEI layer was formed on the substrates by immersing the various substrates in a PEI water solution, and then successively depositing silica on the surface by soaking the LPEI-coated substrates in a silica source solution. The tailored nanosurfaces may have potential applications in the field of liquid transferring, self-cleaning, microfluid, and biomedical-related devices, etc.^[12h-k]

Block copolymer nanoparticles: Block copolymer containing water-soluble polyamine and hydrophobic polymer chains may self-assemble into nano-objects of spherical micelles, worm-like micelles and vesicles in water. These nano-objects composed of a polyamine shell and hydrophobic core are able to direct the formation of duplicated silica and hollow silica by calcination or solvent etching of the organic components. For example, Armes and co-workers^[13] synthesized silica nanospheres with changeable diameter and wall thickness using

a series of amine-based block copolymer spherical micelles or vesicles as templates for biomimetic silica deposition (Figure 8).

Firstly, amine-bearing block copolymer nano-objects were fabricated by the self-assembly process. A certain amount of TMOS as silica precursor was subsequently added into water dispersions. After reaction, hybrids consisting of a polymer core and silica/polyamine shell were obtained with varied diameters from about 20 to 200 nm and wall thickness of about

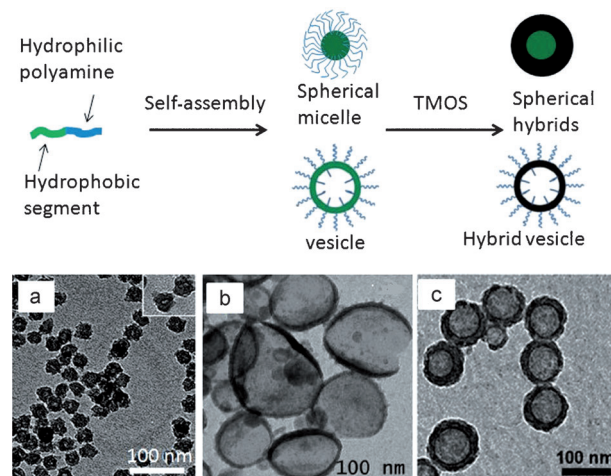


Figure 8. Scheme of silica hybrids obtained by using block copolymer spherical micelles and vesicles as templates and catalyst (top). TEM images of: a) hybrid copolymer-silica particles synthesized using partially quaternized noncross-linked copolymer micelles; b) silicified vesicles formed under the condition of TMOS/amine molar ratio of 10:1 for 8 days; c) silica-coated nanoparticles obtained from a PDMA₁₃₅-PDPA₆₆ diblock copolymer precursor.^[13] Copyright © 2007–2009, American Chemical Society; Copyright © 2009, WILEY-VCH Verlag GmbH & Co. KGaA, Weinheim.

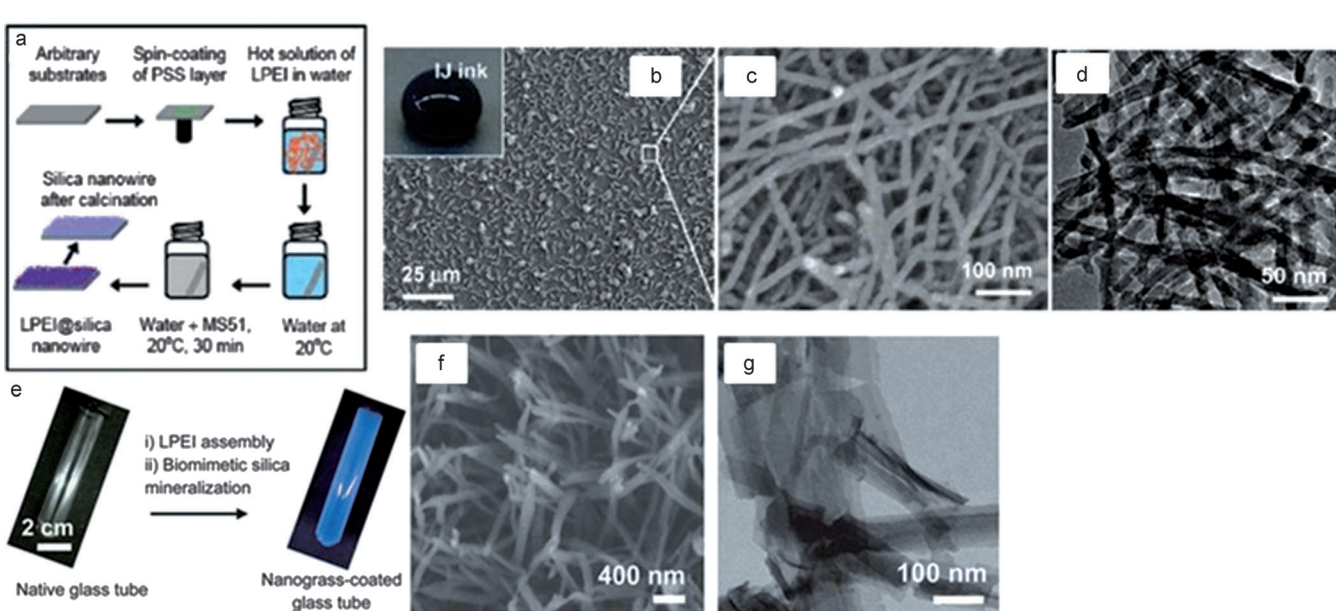


Figure 7. Schematic representation of the bioinspired process on the surface of: a) glass slice, and e) glass tube. b) SEM, and c) its magnification, and d) TEM images of LPEI@silica hybrid nanowires formed on the surface of glass slides. f) SEM and g) TEM images of LPEI@silica nanograss formed on the surface of the tubes.^[12h-k] Copyright © 2011, American Chemical Society; Copyright © 2011, Royal Society of Chemistry.

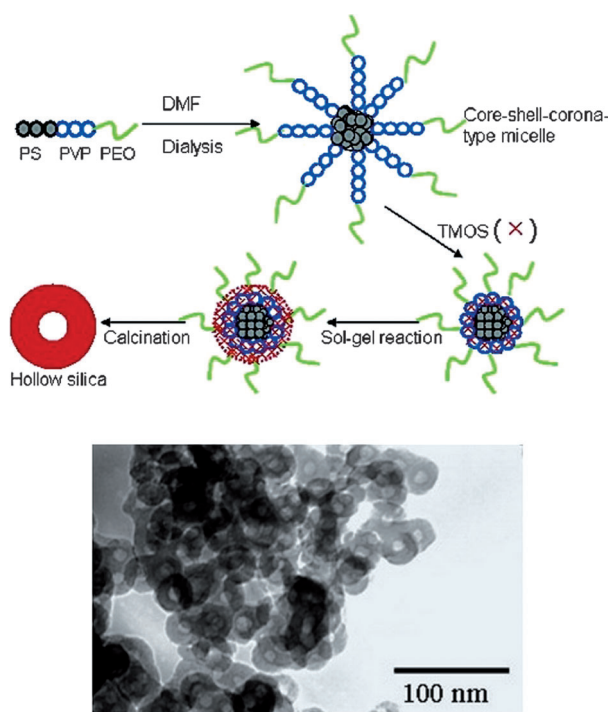


Figure 9. Scheme of the procedure for fabricating hollow silica nanospheres by the sol-gel technique combined with a template of the PS-PVP-PEO micelle (top), and TEM image of hollow silica nanospheres with a uniform size of about 30 nm (bottom).^[14] Copyright © 2007, American Chemical Society.

15 nm. The results demonstrated that all the hybrids appeared uniform in size with stable properties.

Nakashima et al.^[14] used polystyrene-*b*-block-poly(2-vinyl pyridine)-*b*-block-poly(ethylene oxide) (PS-*b*-P2VP-*b*-PEO) triblock terpolymer micelles with a PS core-P2VP shell-PEO corona structure as template to deposit silica for hollow silica nanospheres with a uniform diameter of about 30 nm (Figure 9). In the silicification process, silica precursors selectively reacted in the domain of the P2VP shell and the outer PEO segment protected the micelles from aggregation. Moreover, the silica wall thickness can be controlled by changing the concentration of the inorganic precursor.

In addition, silica-polymer hybrid hollow nanoparticles with channels and gatekeepers were fabricated by the Shi group with thermoresponsive composite micelles of PEG-*b*-PNIPAM and PNIPAM-*b*-P4VP diblock copolymers as template.^[15] A complex micelle with PNIPAM core and PEG/P4VP composite shell was formed when the temperature was lower than the lower critical solution temperature (LCST, ca. 32 °C) of PNIPAM. Then, the structure was fixed by selectively cross-linking P4VP domains in the shell. Silica was then deposited in cross-linked P4VP domains. The PEO-*b*-PNIPAM polymer chain subsequently escaped from micelles by increasing the temperature above the LCST (Figure 10, top). Importantly, these hybrid silica nanoparticles (Figure 10a) may have potential application in the field of controlled drug release (Figure 10b).

Other polyamine-based aggregates: The thermosensitive homopolymer, poly(*N*-isopropylacrylamide) (PNIPAM), was used

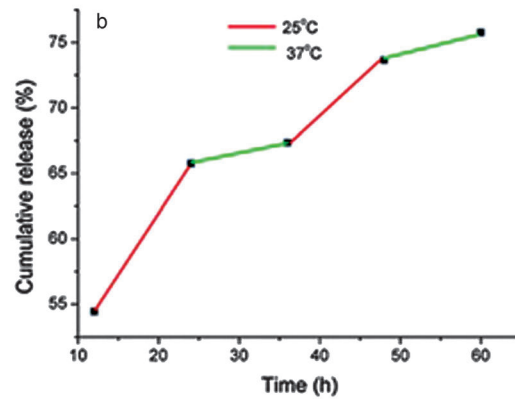
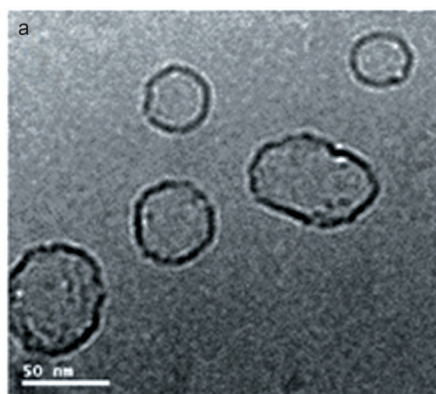
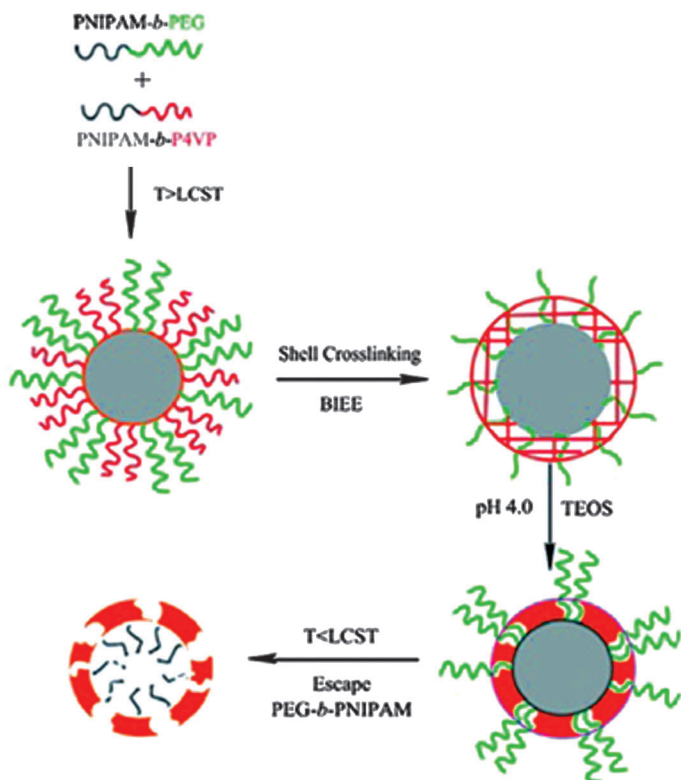


Figure 10. Schematic formation of hybrid hollow nanoparticles with channels in the shells and thermoresponsive gatekeepers using complex micelles as the template (top). a) TEM image of hybrid hollow nanoparticles, and b) cumulative release of doxorubicin from the hybrid hollow nanoparticles at different temperatures (25 and 37 °C) in PBS (pH 7.4, 0.05 M).^[15] Copyright © 2010, American Chemical Society.

as a reversible template to obtain hollow silica nanospheres without the need for further calcination or chemical processing. The thermosensitivity caused PNIPAM chains to collapse to form nanospheres as soft templates for silica deposition at higher temperatures ($>$ LCST), and then PNIPAM with extended free chains diffused out of the cores at lower temperature ($<$ LCST), leading to the formation of hollow silica nanospheres (Figure 11). It is fascinating that the PNIPAM soft templates were recyclable.^[16]

Polystyrene colloids after modification with hairy polyamine were also applied as template to mediate biomimetic synthesis of raspberry-like polymer@silica nanohybrids under ambient conditions. Silica deposition was performed by simply stirring a mixture of the polymeric particles in isopropanol and TMOS in water (Figure 12).^[17,18] The surface structure of the hybrids and the composition of the polyamine–silica hybrid shell could be well controlled by adjusting the silicification conditions.

Single molecular templates

Cylindrical polymer bottlebrushes (CPBs) possess densely grafted polymer side chains from a linear main chain, which causes them to keep an extended conformation in good solvent of side chain polymer. Recently, water-soluble amine-based monomolecular polymer brushes have been developed and used as templates for 1D inorganic matter deposition. Müller and co-workers^[19a] have reported that poly(2-(dimethylamino)ethyl methacrylate)-bearing cylindrical polymer bottlebrushes can be used as single-molecular templates and catalysts for fabrication of uniform silica nanofibers/nanotubes (Figure 13). The 1D silica obtained with such templates have uniform diameter and length, both of which can

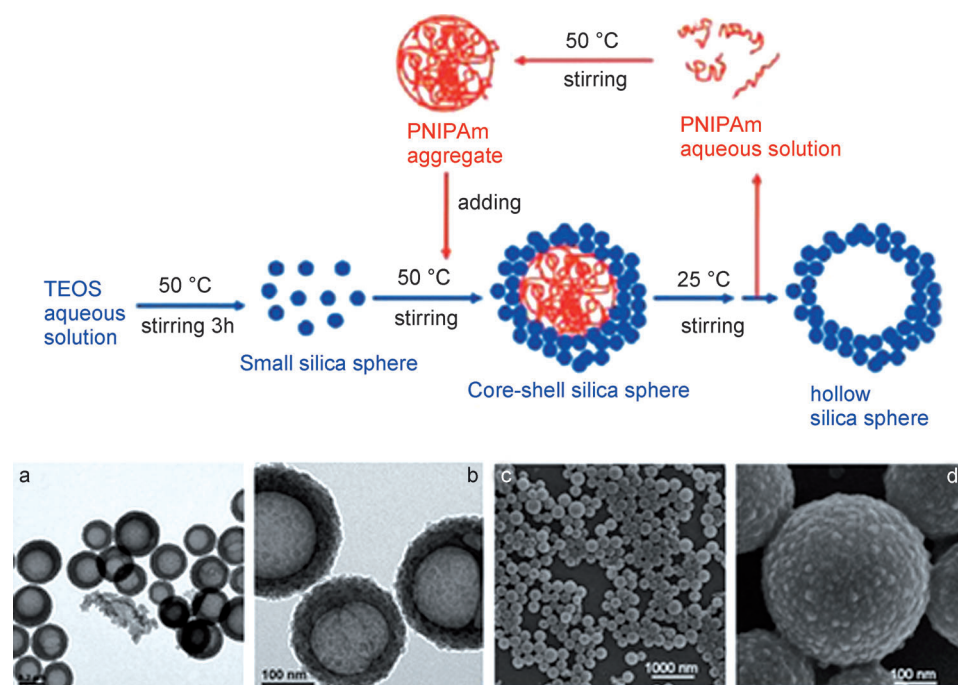


Figure 11. Schematic illustration of the strategy for the one-pot fabrication of hollow silica spheres with a mesoporous shell by using thermosensitive poly(N-isopropylacrylamide) as a recyclable template (top). a), b) TEM, and c), d) SEM images of hollow silica nanospheres obtained with PNIPAM ($M_w = 3.7 \times 10^4$, initial concentration 0.5 wt %) as a template at 50 °C.^[16] Copyright © 2009, American Chemical Society.

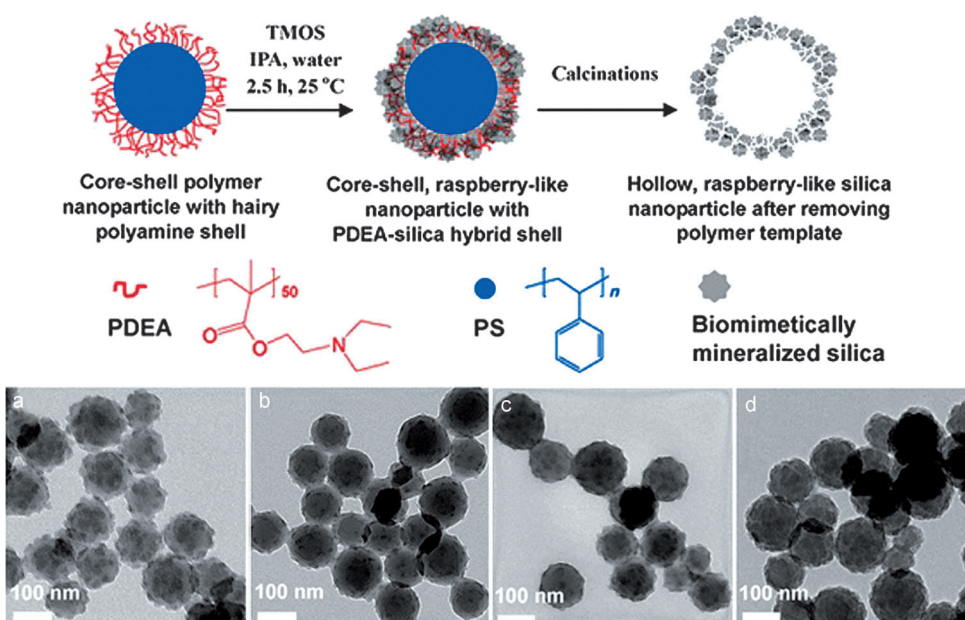


Figure 12. Schematic illustration of the strategy for production of hollow silica nanoparticles (top). TEM images of hybrid polymer–silica nanoparticles with tunable surface morphology: a), b) synthesized by using 100 and 50 µL TMOS in the presence of 1.0 mL water; c), d) prepared using 150 µL TMOS and 0.3 and 0.1 mL of water, respectively; PS-PDEA nanoparticles (2.0 mL) dispersed in IPA (0.25 wt %) were used.^[17] Copyright © 2010, Elsevier.

be accurately adjusted by controlling the composition of the brushes.

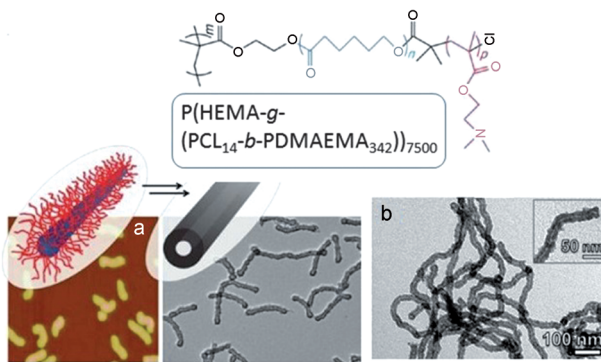


Figure 13. CPB for template (molecular structure top): a) AFM, and b) TEM images of 1D silica nanotubes obtained by template-directed synthesis.^[19a] Copyright © 2012, American Chemical Society.

Silica nano-objects based on sol–gel reaction of polymeric silanes

Siloxane-based polymers with narrow molecular distribution are usually synthesized by controlled radical polymerization technologies, such as atom transfer radical polymerization (ATRP) and reversible addition-fragmentation chain transfer (RAFT) polymerization procedures. Silioxane-bearing polymers and their aggregates have been used to prepare shaped silica nano-objects by hydrolytic condensation under basic or acidic condition. Müller et al.^[19b,c] used polymer bottlebrushes bearing polysiloxane side chains ($\text{P}(\text{HEMA}-g-(\text{PAPTS}_{20}-b-\text{POEGMA}_{57}))_{3200}$) to produce water-dispersed organo-silica hybrid nanowires under catalysis of ammonia (Figure 14). These isolated hybrid nanowires showed good stability in water.

Additionally, Chen et al.^[20] established a versatile methodology for fabrication of core-shell silica hybrids with 0-, 1- and 2-

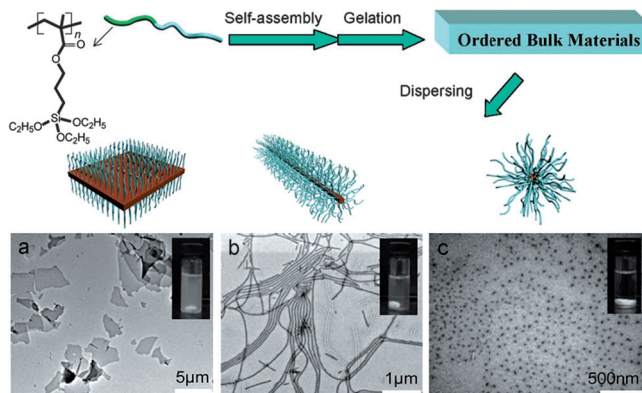


Figure 15. Scheme for preparation (top) and TEM images of functionalized silica hybrid nano-objects with different morphologies: a) nanosheets, b) nanofibers, and c) nanospheres.^[20] Copyright © 2008, American Chemical Society; Copyright © 2013, Elsevier.

dimensional shapes by bulk microphase separation of gelable block copolymers (Figure 15). The shapes of the nano-objects were controlled easily by only changing the composition of block copolymers. Furthermore, these isolated silica hybrids had a quite high density of functional polymer chains tethered on the surface, which provide a sound foundation for application development as carrier and antibacterial materials, and so on.

Peptide-Based Materials as Catalytic Templates

Peptide aggregates and peptide-based block copolymer self-assemblies have also been widely used as templates to direct the biomimetic synthesis of silica structures. Silicas have been obtained with diverse structured morphologies, such as fiber/tube, sphere, plate, nanofiber network and capsule, etc.

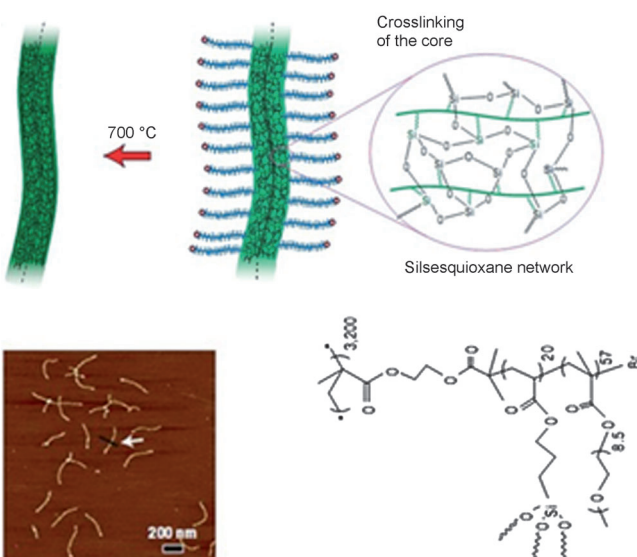


Figure 14. The bottle brush molecular structure and processing scheme of inorganic silica nanowires and AFM height image of inorganic silica nanowires (z range 4 nm) on mica.^[19b] Copyright © 2008, Rights Managed by Nature Publishing Group.

Peptide aggregates

Li et al.^[21a] used poly(L-lysine-HBr) (PLL) homopolypeptides along with phosphate buffer as organic templates to obtain regular hexagonal silica plates, irregular silica nanoparticles, and more complex structures. It was found that mixing sequences, molecular weight and counterion concentrations of polylysine played a key role in terms of controlling the resulting silica morphologies (Figure 16).

In addition, nanotubes have been obtained with peptide fibrils as template by many research groups.^[22–24] For instance, Ansell et al.^[22] selected self-assembled β -sheet peptide nanofibrils as templates for silica nanotubes with the length of hundreds of nanometers and mean pore size of 3.5 nm (Figure 17).

Hollow silica nanotubes with tunable dimensions were also synthesized by Hartgerink et al based on peptide amphiphile nanofiber templates.^[25] It was found that the various peptide amphiphiles showed different catalytic activities for hydrolytic condensation of silica sources, and simultaneously, depending on the reaction conditions and the size of the peptide amphiphile (PA) assembler, the nanotube wall thickness could be varied between 5 and 9 nm (Figure 18).

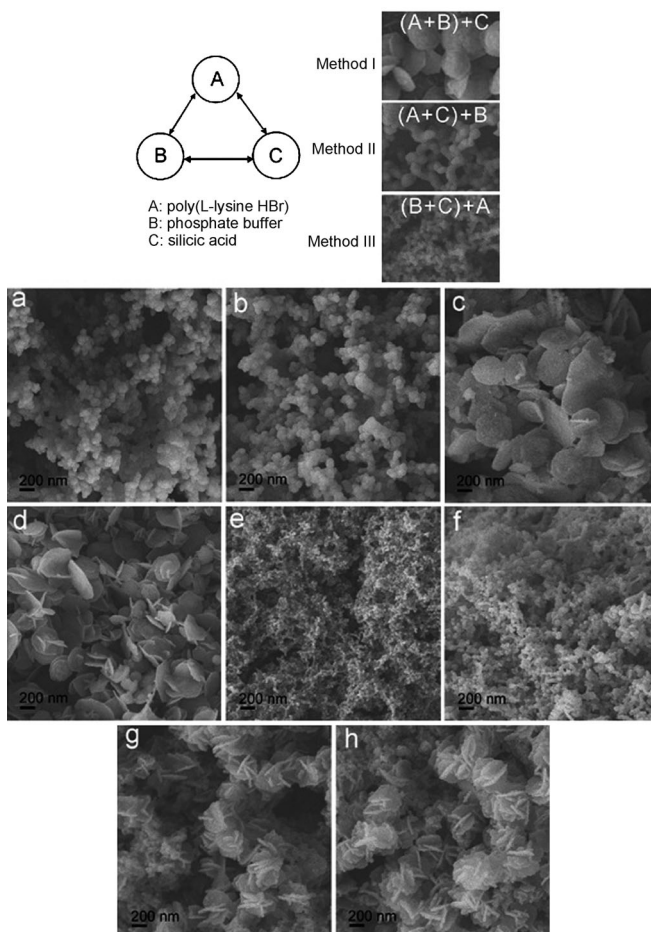


Figure 16. Schematic illustration (top) of the effects of mixing sequences on resulting silica structures and SEM images (bottom) of biosilica produced by: a), b), c), d) poly(L-lysine)₁₄₀, and e), f), g), h) poly(L-lysine)₄₂₀, at different ratios of phosphate/lysine residue: 0.5 (a, e), 1 (b, f), 2.5 (c, g), 5 (d, h).^[21a] Scale bars: 200 nm. Copyright © 2011, American Chemical Society.

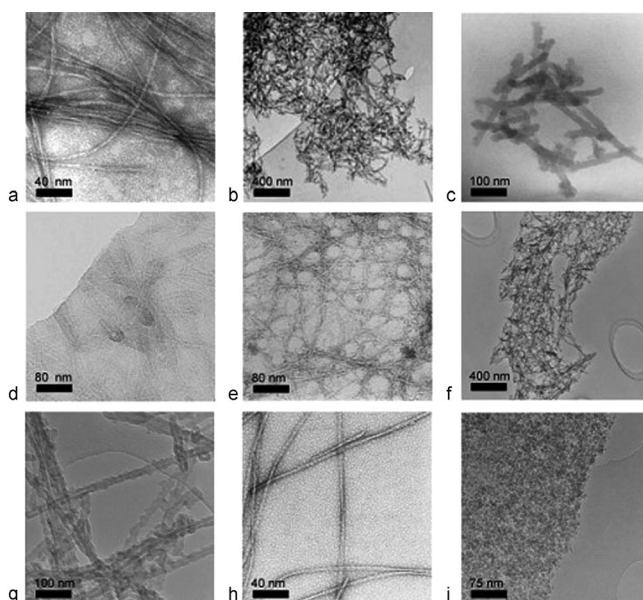


Figure 17. TEM images of: a), b), c) β-sheet peptide fibrils, and b), c), e), f), g), i) silica hybrids templated by peptide fibrils with different stoichiometric ratios.^[22] Copyright © 2004 WILEY-VCH Verlag GmbH & Co. KGaA, Weinheim.

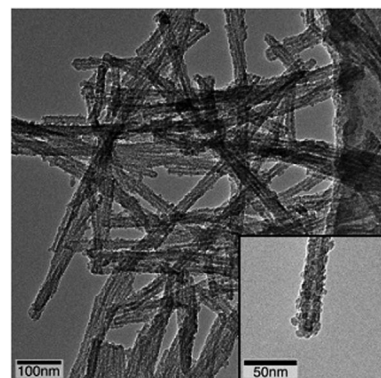


Figure 18. TEM image of silica-coated PA samples after incubation in TEOS. [TOES]/[PA] = 100; 7 days incubation.^[25] Copyright © 2007, American Chemical Society.

Also, self-assembling peptides with hydroxyl groups adjacent to free amine functionalities have been used for targeted templating of silica material.^[26] Silica-binding peptide nanofibrils were obtained by incubating TMOS with peptide fibrils with amino terminal groups for 15 h (Figure 19). Finally, fibrous silica with humps on the surface were obtained.

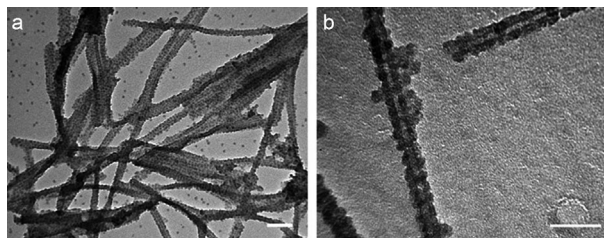


Figure 19. a) NH₂-NSGAITIG-CONH₂ peptide fibrils after incubation with TEOS for 15 h (scale bar: 100 nm). b) Closer magnification of a fibril templated with silica particles (scale bar: 50 nm).^[26] Copyright © 2011 Wiley Periodicals, Inc.

Silica hybrid networks were also formed with interconnected, self-assembled β-sheet peptide fibrils as template (Figure 20). The mechanical characteristics of these hybrid networks can be modulated by changing the stoichiometric parameters of the sol-gel process.^[27]

In addition, the utilization of polypeptide secondary structures as a means of controlling oxide pore architectures was explored by Shantz et al.^[28] It was found that silica synthesized with poly-L-lysine in an α-helix conformation possessed cylindrical pores with the size of 1.5 nm, whereas larger pores appeared when using poly-L-lysine in the β-sheet conformation.

Self-assemblies of peptide-based block copolymer

Recently, researchers also fabricated a series of silica nanomaterials templated by peptide-bearing diblock copolymer self-assemblies. For example, Li et al.^[21b,c] used a double hydrophilic block copolymer poly(ethylene glycol)-block-poly(L-lysine)

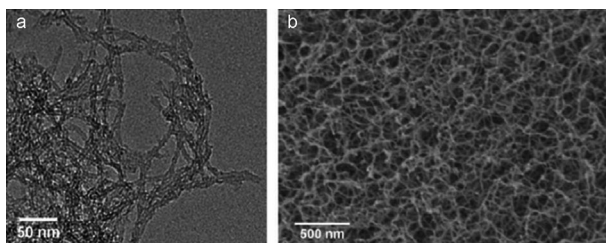


Figure 20. a) TEM image of silica-coated MAX8 peptide fibrils showing dark silica shell encasing a light core of the peptide fibrils; and b) cryo-SEM image of silicified MAX8 fibril network.^[27] Copyright © 2010, American Chemical Society.

(PEG-*b*-PLL) and an amphiphilic diblock copolypeptide of poly(L-lysine-HBr)-*b*-block-poly(L-leucine) (KL) as templates to prepare silica, and further explored the parameters leading to changes in the silica shape (Figure 21, Figure 22 and Figure 23).

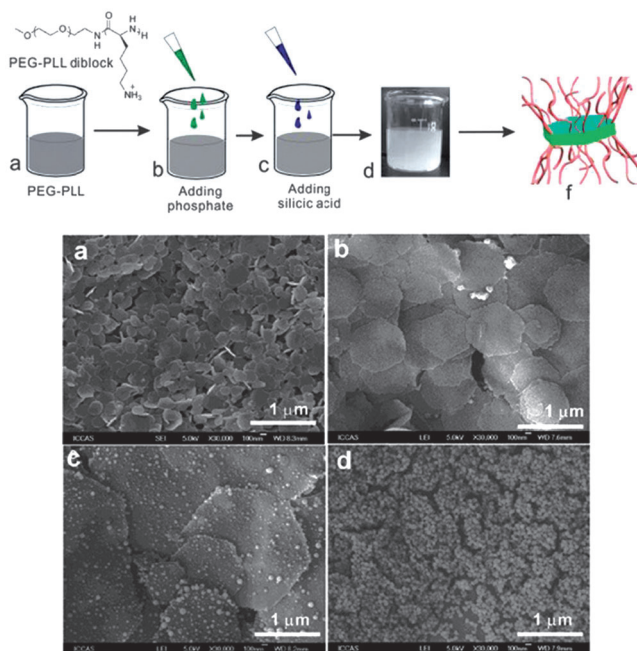


Figure 21. Schematic illustration for synthesis of silica nanoplate (top) and SEM images of silica hybrids templated by PEG₄₅-*b*-PLL₁₀₀: a) [Si]/[NH₃⁺] = 10, [phosphate]/[NH₃⁺] = 5; b) [Si]/[NH₃⁺] = 20, [phosphate]/[NH₃⁺] = 5; c) [Si]/[NH₃⁺] = 100, [phosphate]/[NH₃⁺] = 5; and d) [Si]/[NH₃⁺] = 20, phosphate/[NH₃⁺] = 1.^[21b] Copyright © 2012, Royal Society of Chemistry.

As shown in Figure 21, hexagonal silica nanoplates with different sizes and irregular silica spheres based on self-assemblies of PEG-*b*-PLL as templates were produced by adjusting the ratios of [phosphate]/[NH₃⁺] and [Si]/[NH₃⁺]. Silicas were obtained with the structures of hexagonal platelets, rods, and fused platelets by using KL block copolymer self-assemblies as template. The shapes were adjusted by changing the chain length of the KL diblock and type of counter ions (Figure 22 and Figure 23).

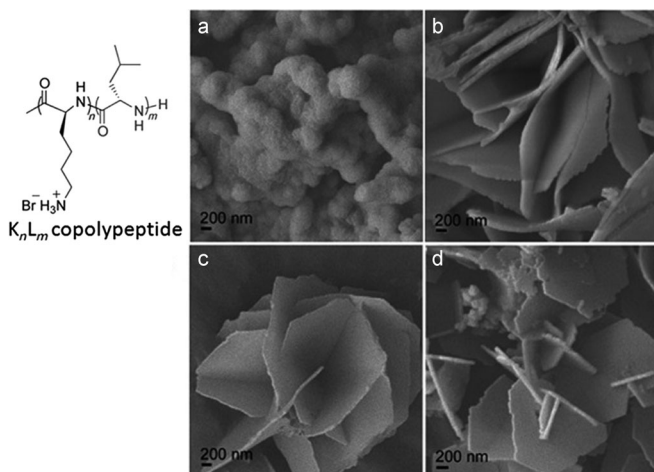


Figure 22. Effects of copolypeptide molecular weight and composition on biosilica structure. SEM images of biosilica directed by: a) K₂₀₀L₂₀; b) K₃₄₀L₂₀; c) K₃₈₀L₁₅; and d) K₄₄₀L₃₀ diblock hydrogels. The copolypeptide concentration is 1 wt %, and the counterion is phosphate.^[21c] Copyright © 2010 WILEY-VCH Verlag GmbH & Co. KGaA, Weinheim.

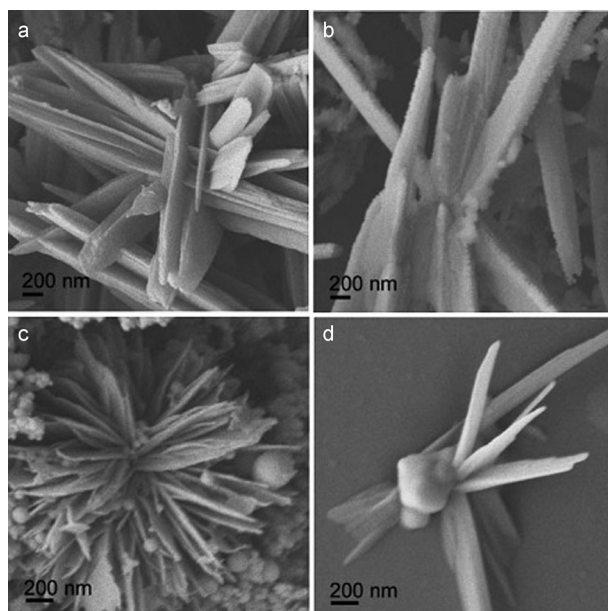


Figure 23. Effects of counter ions towards K₄₄₀L₃₀ templated biosilicification. SEM images of K₄₄₀L₃₀-directed silica structures using sulfate as the additive anion: a) before calcification, and b) after calcification. SEM images of K₄₄₀L₃₀-directed silica structures using carbonate as the additive anion: c) before calcination, and d) after calcination.^[21c] Copyright © 2010 WILEY-VCH Verlag GmbH & Co. KGaA, Weinheim.

In addition, Mastai et al.^[29] selected diblock copolymer of poly(ethylene oxide)-*b*-block-poly(D-phenylalanine) (PEO-*b*-D-Phe) as a surfactant template to obtain chiral mesoporous silica materials with highly ordered periodic structures of hexagonal symmetry, and with a pore size of about 5 nm and high surface area of about 700 m² g⁻¹ (Figure 24). It was found that this material had potential application for enantioselective separation.

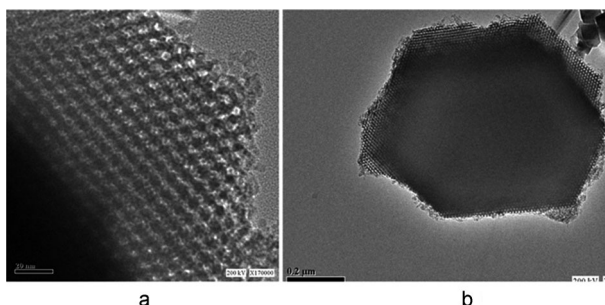


Figure 24. TEM images: a) high resolution b) low resolution of chiral silica made from PEO₁₁₃-*b*-D-Phe₁₀ after chiral copolymer extraction. The light areas correspond to the pores, whereas the dark areas correspond to the walls.^[29] Copyright © 2007, American Chemical Society.

Chiral Templates for Transcribing Chirality into Silica Materials

The self-assembled structures of amphiphilic molecules are attractive candidates for utilization as organic templates due to their various shapes and the controllable kinetics of their supramolecular aggregates. Especially, the formation of various amorphous silicon oxides, such as vesicle-like morphologies,^[30–32] pillar-like structures,^[33] tubular and wire-like structures,^[34–36] through the use of various methods, such as sol-gel polycondensation from supramolecular structures of amphiphiles as template, have been reported.

In conventional sol-gel polycondensation, typically, silicon alkoxides (Si(OR)₄) are preferentially employed as silica precursor since they can be easily changed to a negatively charged form after prehydrolysis. To control sol-gel process, acceptors with sites of amines and positive charges must be available. Thus, cationic surfactants based on quaternary ammonium have been frequently used as organic template.^[37] The driving force of organization is the presence of cationic charges on the amphiphiles, resulting in the containment of anionic silica precursors on contact with the surface of the bilayer. By addition of aminosilane or quaternized aminosilane as a co-structure-directing agent (CSDA), anionic surfactant can be also used for organic templates.^[38–40] In this sense, chirality provided by amphiphilic molecules would be appropriate for constructing chiral silica by the conventional sol-gel reaction.

Chiral silica by sol-gel reaction

Similar to the usually-templated silica, chiral silica morphologies based on the organic template of self-assembled chiral amphiphiles can also be tuned by various factors, such as mechanical strength, and control of the kinetics of the sol-gel transcription process by physical or chemical properties. In 2000, Shinkai and co-workers first reported chiral silica morphologies obtained by sol-gel polycondensation mediated by chiral organogels.^[41,42] Cholesterol-based gelators can often form helical or tubular structures in organic solvents, which can be transcribed directly to chiral silica fibers with keeping their shapes (Figure 25). The organogel of divebzi[30]crown-10 derivative **1** in acetic acid provided tubules and helical ribbon

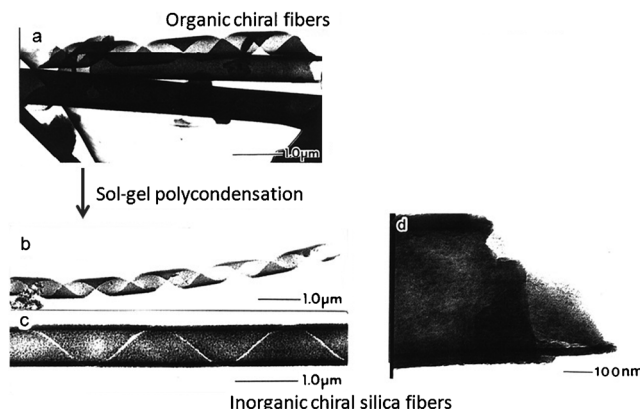
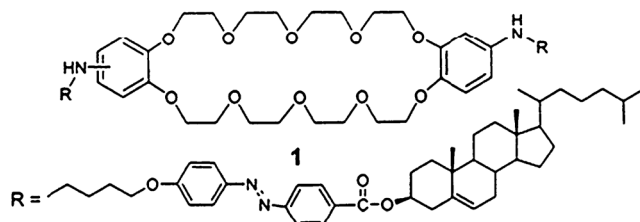


Figure 25. TEM images of: a) helical and tubular fibers as organic templates, b), c), d) chiral silica structures after calcination obtained by sol-gel polycondensation.^[42] Copyright © 2001, American Chemical Society.

structures (Figure 25 a). Transcription was carried out in the presence of benzyl amine because of two amino moieties which were protonated in acetic condition; as a result, the corresponding chiral silica fibers were obtained (Figure 25 b and c). Both organic and silica structures were right-handed helical motifs, which indicated that the microscopic helicity is reflected by the macroscopic helicity. Interestingly, Figure 1 d shows double layers with an interlayer distance of 8–9 nm in silica fibers after calcination (Figure 25 d), which resulted from the removal of organogel that was acting as the template during the polycondensation.

After this work, many chiral silica materials were synthesized by sol-gel transcription using self-assembled supramolecular fibers as organic templates. For example, well-defined double-helical silica nanotubes with a diameter of 50 to 80 nm and a pitch of 500 to 600 nm, the structures of which were quite similar to double-helical DNA, were obtained through the hydrogel of double-helical superstructures from sugar-based amphiphiles (mixture of **2** + **3**) in water/methanol as organic templates (Figure 26).^[43]

More recently, studies of chiral silica with tunable shape, size and helicity, during the transcription of organic helical aggregates into inorganic helices have been reported. The work on sol-gel transcription of silica morphologies obtained by gel network of cationic bisquaternary ammonium gemini surfactants **4** with tartrate counter-anion began in early 2000 with a collaboration between the groups of Oda and Shinkai. They successfully transcribed chiral ribbons based on self-assemblies for which the chirality was controlled by enantiomeric excess (ee) of organic molecules (ee = 1 means pure enantiomer with gemini L-tartrate). The replication protocol used in this work

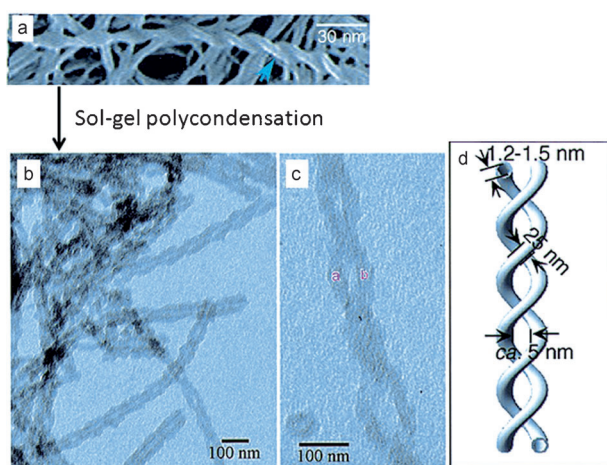
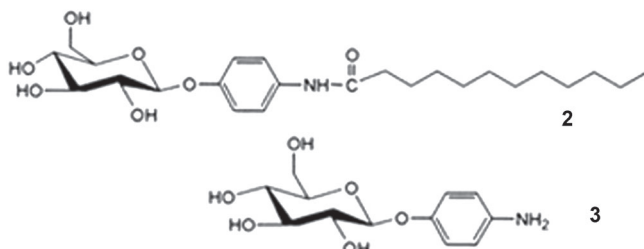


Figure 26. a) FE-SEM image of the hydrogel prepared from the mixed gel 2 and 3 in water/methanol. b), c) TEM images of double-helical silica nanotubes after calcination, and d) schematic representation of double-helical structure of silica nanotubes.^[43] Copyright © 2002, American Chemical Society.

consisted of mixing the gemini surfactants and the silica precursor (TEOS, 4.6%) in the presence of benzylamine (2.3%) as catalyst in a mixture of water/pyridine (1:1). When the ee was decreased from 1 to 0.2, the twist pitches of inorganic fibers increased (Figure 27).^[44] However, these twist pitches were smaller than the organic twisted ribbons because shrinkage of silica fibers may have occurred during the calcination process.

A few years later, Delclos et al. reported the detailed study on the morphological control of the hybrid gemini–tartrate system. They have shown that not only can the twist pitch of these hybrid nanosystems be controlled by ee, but also their shapes are tunable between twisted, helical ribbons or tubes.

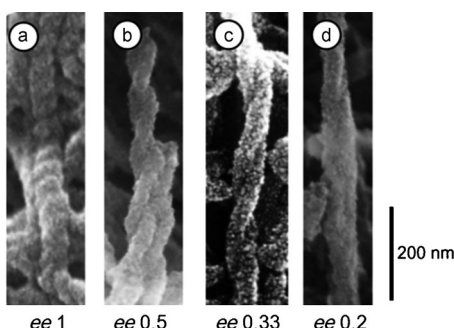


Figure 27. SEM images of chiral silica fibers with different helical pitch obtained by varying ee of gemini tartrate gel as organic templates.^[44] Copyright © 2002, Royal Society of Chemistry.

Various parameters, such as temperature, solvent or reactant concentrations, can have distinct and opposite effects on their structures. They have also shown that both the relative kinetics of the organic assembly formation and the inorganic polycondensation have remarkable effects on the final morphologies of the inorganic nanostructures.^[45] As an example, the TEM images of the organic tubes and their silica nanoreplicates illustrating how the morphologies of silica replicates strongly depend on the aging time of the organic template are shown in Figure 28. Only 3 days were needed for the organic gels to

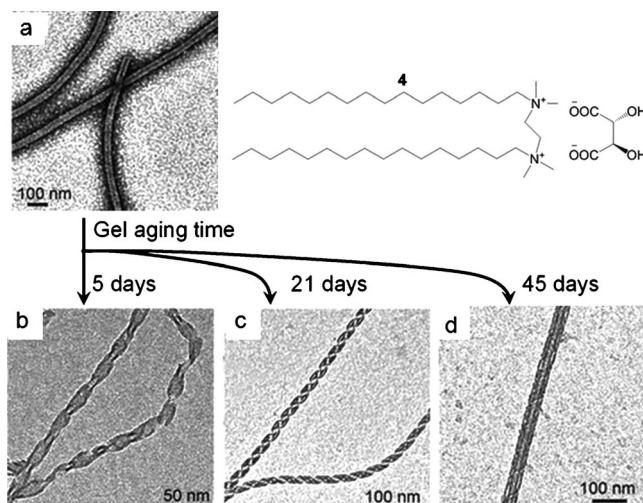


Figure 28. TEM images of the morphology of inorganic ribbons obtained by transcription of organic 16-2-16-L-tartrate gels obtained under different conditions. Particularly aging times of organic gels can affect the shapes, such as twisted (5 days), helical ribbons (21 days), and tubes (45 days).^[45] Copyright © 2008, American Chemical Society.

form organic nanotubules, however, it should be noted that 5 day aged organic gel transcribed into twisted ribbons (Figure 28b) whereas 21 day aged ones underwent a morphological change to helical silica ribbons (Figure 28c). It was only when the gels were aged for longer than 45 days that the resulting inorganic fibers kept their tubular structures (Figure 28d). The average diameter of an inorganic helix is 25 nm, and the length is of the order of micrometers.

These results show that the extremely flexible nature of **4** hydrogel exhibits not only a rich polymorphism of supramolecular assemblies but also different stages of evolution from one structure to another, which allows fine-tuning not only of the morphologies of organic templates but also of the structure of the inorganic replica.

Huang et al. have successfully fabricated single- and double-helical silica nanofibers by using single-chain amphiphile **5** composed of butyl, azobenzene group, and sugar moiety as organic template and TEOS silica precursor.^[46] Generally **5** can self-assemble to form double-stranded nanohelices in aqueous solution through noncovalent interactions (Figure 29a); these nanohelices were exclusively left-handed with a pitch of approximately 25 nm and a diameter of 14–16 nm. Therefore, these nanohelices can act as soft templates to create double-

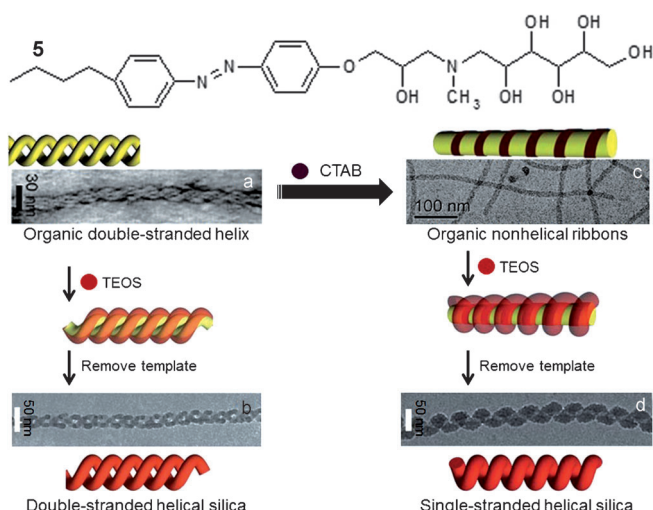


Figure 29. Schematic illustrations and TEM images of: a) the organic double-stranded helix from amphiphile 5, and b) double-stranded helical silica templated from amphiphile 5; c) nonhelical ribbons of 5/CTAB solution, and d) single-stranded helical silica obtained by achiral structure.^[46] Copyright © 2010, American Chemical Society; Copyright © 2011, Royal Society of Chemistry.

stranded silica nanofibers (Figure 29 b). Upon decoupling the double helices of 5 with cationic surfactant, such as cetyltrimethylammonium bromide (CTAB), double-stranded helical fibers were destroyed and transformed to nonhelical structures (Figure 29 c) with a decrease in the Cotton coupling of CD spectra because CTAB caused interchained repulsion of hydrogen bonds. In an interesting twist, these nonhelical nanofibers can be utilized as soft templates to create single-stranded silica nanohelices with high yields, which show a width of 40–50 nm and pitch of 30 nm with a more distended structure than double-stranded helical silica (Figure 29 d). In this case, the silica source might be adsorbed to the single helical organic template by electrostatic force between the positively charged CTAB.

The above-described examples show all chiral silica structures that were obtained by sol-gel polycondensation of TEOS precursor with soft templates of self-assembled chiral supramolecular morphologies which could well-define the morphologies of organic fibers. Furthermore, the silica structures were finely tuned by controlling the kinetics of transcription or external factors.

Chiral silica with ordered mesoporous structure

At the other extreme, chiral mesoporous silica have also been investigated by many researchers. In 2004, Che et al. presented the first synthesis of chiral silica with ordered mesoporous structures using L-amino acid-based surfactant as template, TEOS and aminosilane as inorganic sources.^[47] The main feature of this approach was controlling the micelle head-group interaction between *N*-miristoyl-L-alanate sodium salt (C_{14} -L-AlaS) as chiral anionic surfactant, including a small amount of free amino acid *N*-miristoyl-L-alanine (C_{14} -L-AlaA) as a co-surfactant and quaternized aminosilane or aminosilane as a CSDA.

The positively charged ammonium site of *N*-trimethoxysilylpropyl-*N,N,N*-trimethylammonium chloride (TMAPS) or 3-aminopropyltrimethoxysilane (APS) interacted electrostatically with the negatively charged head-group of C_{14} -L-AlaS or C_{14} -L-AlaA (Figure 30). The trimethylene groups of TMAPS and APS were covalently bonded with TEOS and subsequently formed the silica framework.

Figure 31 shows the morphology and mesostructure of a typical chiral mesoporous silica (CMS), which was characterized by XRD, SEM and TEM. The XRD pattern exhibited three well-resolved peaks in the range $2\theta = 1.5\text{--}6^\circ$, which could be indexed as 10, 11 and 20 reflections based on the 2D hexagonal $p6mm$

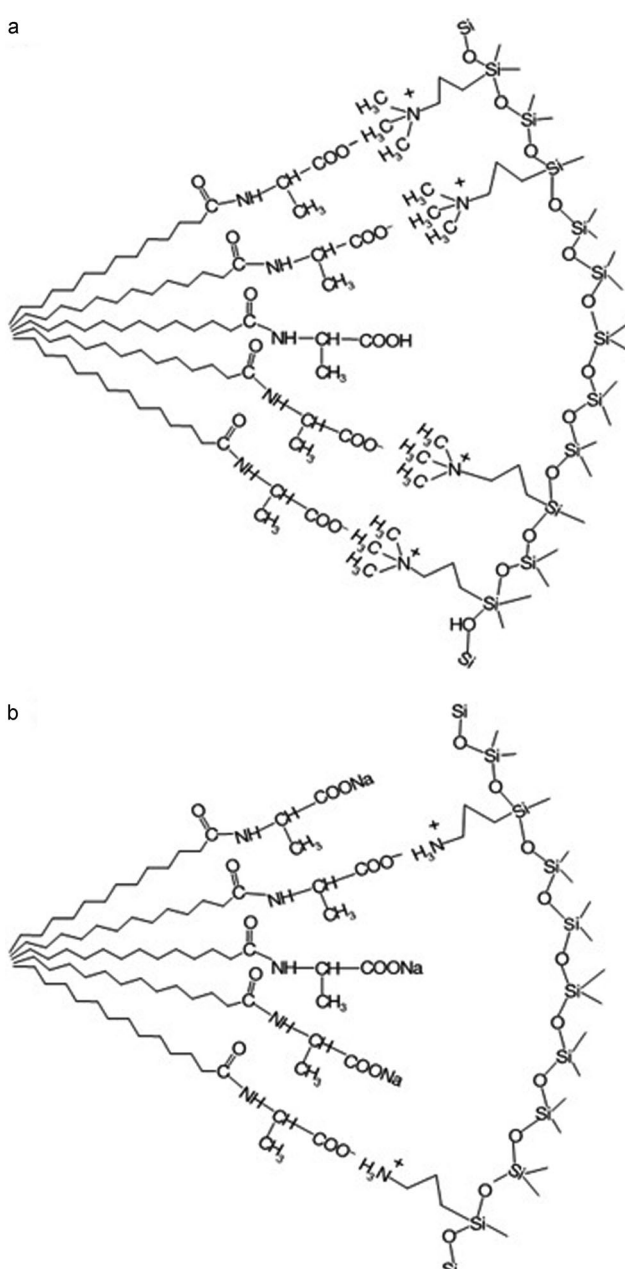


Figure 30. Schematic illustration of two type of interaction: a) C_{14} -L-AlaS and TMPS, and b) C_{14} -L-AlaA and APS.^[47] Copyright © 2004, Rights Managed by Nature Publishing Group.

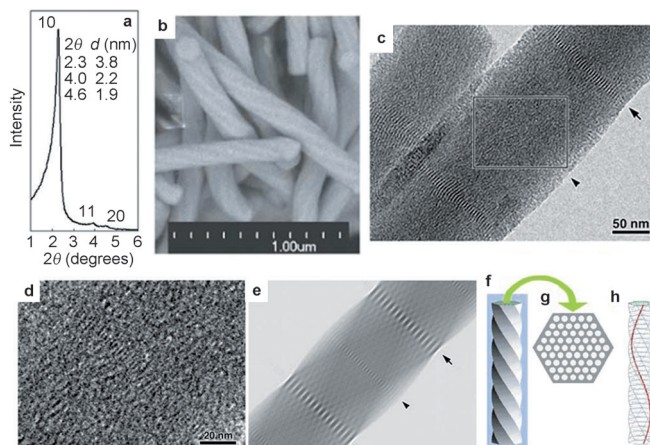


Figure 31. a) XRD pattern, b) SEM image, and c) TEM image of a typical CMS structures. d) Enlarged image of the selected area in (c), and e) a simulated TEM image. Schematic illustrations of: f) corresponding chiral mesoporous material, g) cross-section, and h) chiral channels in the materials.^[47] Copyright © 2004, Rights Managed by Nature Publishing Group.

unit cell (Figure 31 a). The SEM results indicated a twisted rod-like hexagonal morphology with 130–180 nm in the outer diameter, approximately 1–6 µm in length, and about 1.5 µm in helical pitch (Figure 31 b). The SEM image provided the external morphology, but did not confirm the existence of chiral pore structures inside the rods. However, 2D projected TEM image (Figure 31 c and d) and simulated image (Figure 31 e) clearly show 2D hexagonal chiral channels running inside the rod. Results of both XRD and TEM analysis indicated that the mesoporous silica have a highly ordered hexagonal mesoscopic structure in conjunction with 2D chirality which was running inside and parallel to the ridge edge (Figure 31 f–h).

A few years later, Che and co-workers demonstrated how to control the morphology of CMS inorganic architecture. Shape and size control were achieved by various stirring rates during sol-gel polycondensation (Figure 32).^[48] When the stirring rate was lower than 300 rpm, the sample showed various twisted ribbon-like structures and the length of hexagonal rods ranged from several micrometers to 20 µm and the outer diameters varied from 50 nm to few hundred nanometers. By increasing the stirring rate, the morphologies became uniformly twisted rod-like with a hexagonal cross-section and the length of the rods decreased whereas their diameter increased. This suggested that stirring could be used as a convenient tool for controlling not only the size and shape of chiral particles but also the chiral structure and helical pitch length for preparation of inorganic architectures.

Following the work of Che, an enormous number of CMS morphologies have been reported. Some examples are summarized in Figure 33. Figure 33 a shows beautiful helical fibers of silica with pore channels running inside the rod, but surprisingly, these structures were organized by an achiral cationic surfactant CTAB.^[49] These helical silica fibers were synthesized under acidic conditions with two phase systems (H_2O , CTAB, HCl for the aqueous phase and TEOS in hexane for the oil phase), and possessed two levels of helical structures: 1) the

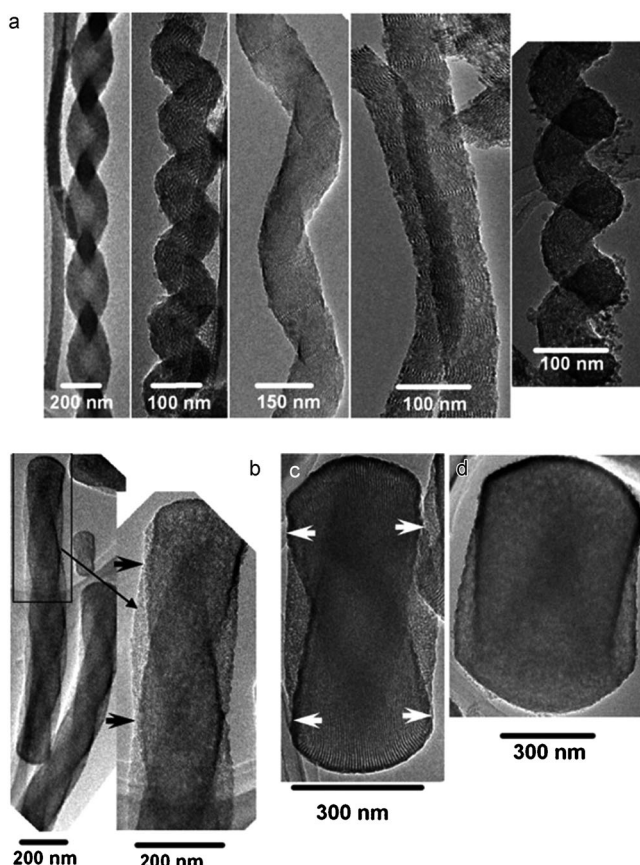


Figure 32. TEM images of chiral mesoporous silica synthesized at various stirring rates: a) 200, b) 400, c) 600, and d) 800 rpm.^[48] Copyright © 2006 WILEY-VCH Verlag GmbH & Co. KGaA, Weinheim.

twisted hexagonal morphology with chiral mesochannels winding around the fiber axis, and 2) these twisted hexagonal nanofibers could further curve spirally to form higher-ordered helical morphology. The hierarchically helical morphology of these nanofibers from an achiral system could be explained by different kinds of topological defects^[50] existing in the silicate liquid crystal seeds which were formed in a diffusion-controlled process, and defects could initiate and direct the growth of particular forms of mesostructured silica.

Yang et al. demonstrated the preparation of ethylene-silica nanofibers with chiral pore channels inside and lamellar pores on the surface shown in Figure 33 b.^[51] This hybrid material was prepared using CTAB and (S)-β-citronellol as CSDA under basic conditions. These nanofibers contained left- and right-handed helices with 2.0 µm in length, 100–200 nm in diameter and about 0.1 µm in helical pitch. Lamellar mesopores were identified with FESEM images (Figure 33 b2), which were formed by merging the hexagonally arranged cylinder-like silica/surfactant micelles. TEM images clearly show many fringes within a single nanofiber and arranged pore channels in a hexagonal symmetry (Figure 33 b3 and b4).

Figure 33 c shows branched CMS nanoribbons which were fabricated through a dynamic templating process using self-assemblies of amino acid-based L-16Phe6PyBr amphiphiles.^[52] These amphiphiles could self-assemble to form short ribbons

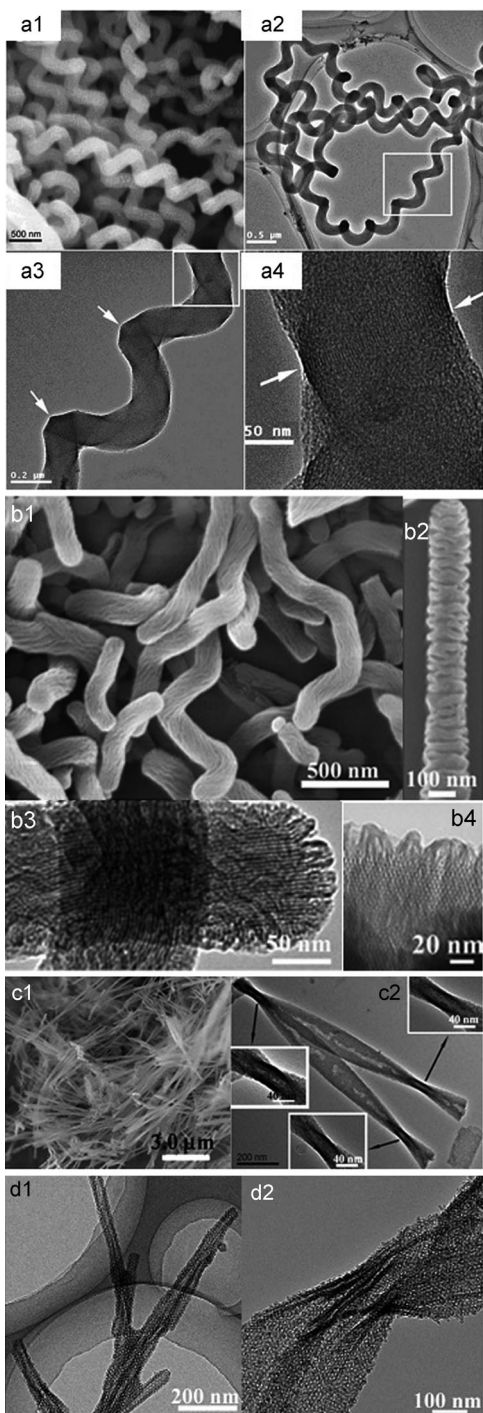


Figure 33. Various helical silica structures. a) Mesostructures nanofibers with higher-order helical morphology.^[49] b) Ethylene-silica nanofibers with chiral and concentric circular pore channels.^[51] c) Branched mesoporous silica nanoribbons.^[52] d) Coiled silica nanoribbons with mesopores in the wall.^[53] Copyright © 2006, 2008, 2010, Royal Society of Chemistry; Copyright © 2010, American Chemical Society.

and fibers with μm size floating in a mixture of 1-propanol and water, and then sol-gel transcription was carried out to form the branched silica nanostructures. These silica nanoribbons were left-handed twisted with a uniform helical pitch of $3.0\ \mu\text{m}$. The TEM image clearly shows the running of lamellar

pore architectures with a width of $4.0\ \text{nm}$ as determined by nitrogen adsorption-desorption measurements.

Single-handed coiled silica nanoribbons with mesopores in their walls were prepared by a dual-templating approach using a mixture of amino acid-based low molecular weight amphiphiles and triblock copolymer as organic templates, and TEOS as silica precursor (Figure 33 d).^[53] The obtained structures were left-handed coiled nanoribbons. TEM images clearly show mesopores on their surface, which are finely organized in a 2D hexagonal-like structure. These mesoporous silica nanoribbons were approximately $200\text{--}400\ \text{nm}$ in width, $25\ \text{nm}$ in thickness, and $5.0\text{--}6.0\ \text{nm}$ in diameter of the mesopores. From the result of N_2 sorption measurements, the BET surface area of these nanoribbons reached $700\ \text{m}^2\text{g}^{-1}$, which is much higher than other silica fibrous materials (normally lower than $200\ \text{m}^2\text{g}^{-1}$).

The synthesis methods of the chiral silicas described above are still in the regime of conventional sol-gel reaction because the chiral templates themselves do not promote the polycondensation. Silica formation often needs additional achiral catalysts, such as acidic or basic compounds. The common point in the above chiral silicas is helical appearance. However, helical silica are also available in the presence of achiral templates since helix formation is an entropy-driven self-assembly process.^[54] Therefore, the helical structure appearance in silica morphology is not essential to chirality.

Biomimetic silica with chirality

As mentioned above, in biomimetic silica synthesis many organic matrices themselves not only act as templates but also as catalysts for the silica deposition, which is different to the conventional sol-gel reactions. Among the organic matrices, in practice, chiral peptides have often been used as catalytic templates for silicification to produce nanoscaled tubular silica. Therefore, we could guess that the chirality would be imparted to the corresponding silica nanotube although there were no microscopically visualizable helical structures. Unfortunately, studies on chiral polypeptide-templated silica have only focused on silica morphology control but ignored the chirality of the resulting silica.

Recently, we expanded our PEI/water-based biomimetic silica design program to PEI/chiral-acid-based chiral silica construction. Based on the fact that PEI easily interacts with guest water to form nanosized crystallites with the 1:2 molar ratio of EI unit/water, we focused our attention on the interactions between achiral PEI (base) and chiral dicarboxylated compounds. We found that PEI interacted with guest chiral tartaric acid or glucaric acid in a 1:1 molar ratio of NH/COOH to form nanoscale crystalline complexes, which exhibited evident CD activity in solid state.^[55,56] We employed chiral or racemic crystalline complexes consisting of linear PEI and chiral D-, L-, and DL-tartaric acid as templates to deposit silica in the same way as we did in the PEI/water system. Expectedly, all templates easily produced silica hybrids $\text{SiO}_2/\text{PEI@D}$, $\text{SiO}_2/\text{PEI@L}$ and $\text{SiO}_2/\text{PEI@DL}$ under very mild conditions of ambient temperature, nearly neutral aqueous medium and short reaction time.^[55] The three hybrid materials were investigated by solid-state diffuse reflec-

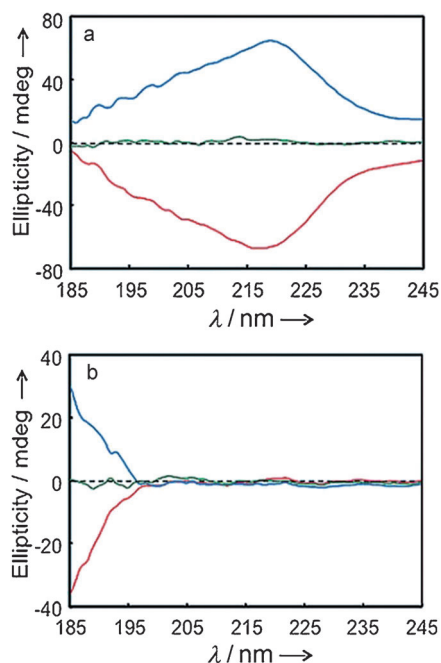


Figure 34. DRCD spectra of silica materials SiO_2/D (red), SiO_2/L (blue) and SiO_2/DL (green); a) before, and b) after calcination.^[55] Copyright © 2012 WILEY-VCH Verlag GmbH & Co. KGaA, Weinheim.

tance circular dichroism (DRCD) spectroscopy (Figure 34). Before calcination, the chiral hybrid of $\text{SiO}_2/\text{PEI@D}$ and $\text{SiO}_2/\text{PEI@L}$ each showed an intense negative and positive ellipticity peak around 218 nm, respectively, while $\text{SiO}_2/\text{PEI@DL}$ did not (Figure 34a). After calcination at 600 °C, surprisingly, the CD signs of each chiral silica material SiO_2/D and SiO_2/L remained

and shifted to shorter wavelength (180–190 nm), arising from SiO_2 absorption (Figure 34b). This result indicates that the silica wall was imprinted with the chirality from chiral crystalline templates. We confirmed that the chiral silica wall was capable of maintaining its chirality even after treatment at 900 °C.

Furthermore, when achiral chromophores, such as PhSiO_3 , porphyrin, and gold nanoparticles were covalently bound or physically adsorbed onto calcined chiral silica, the achiral chromophores showed negative ellipticity signals for SiO_2/D and positive ellipticity signals for SiO_2/L in their absorption bands (Figure 35).^[55] These surprising phenomena probably occurred by the existence of considerable interactions between chiral silica wall and achiral guests, which led to the induction of chirality to achiral guests including molecules and metal nanoparticles. This feature would be potentially applicable in sensing and remoting field.

Replacing the chiral source of tartaric acid by D -glucaric acid, we also developed chiral crystalline complexes consisting of PEI and D -Glc (PEI/ D -Glc) and used this complex as catalytic template in the hydrolytic condensation of TMOS (Figure 36). Interestingly, the complex PEI/ D -Glc showed nanosheet structures with crystallites and promoted the silicification of TMOS to direct chiral silica with nanosheet-stacked morphology.^[56] Tuning the formation conditions of the template of PEI/ D -Glc by pH and metal ions, such as Ca^{2+} , Zn^{2+} , Mg^{2+} , we controlled the silica nanosheet array with spherical or twisted structures (Figure 37). After calcining and introducing some organic residues, such as phenyl, naphthalene, anthracene to the silica nanosheets, the guests' molecular residues showed induced CD activity reflecting the status of $\pi-\pi$ interactions between guest residues on the chiral silica nanosheets.

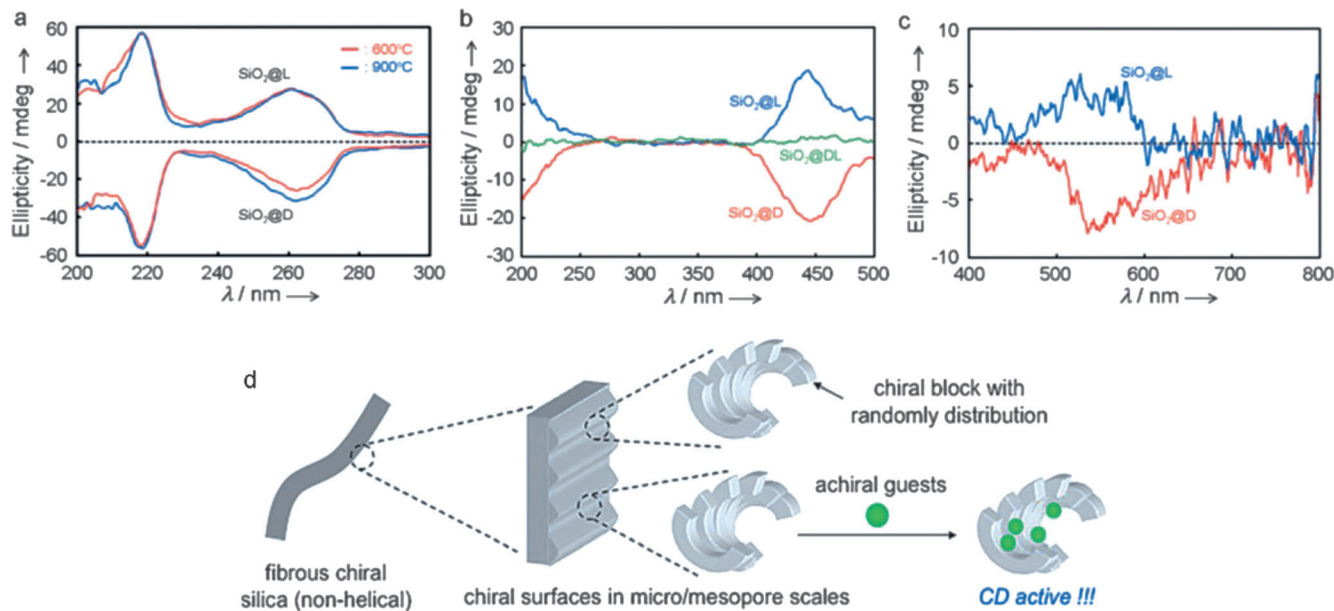


Figure 35. Induced DRCD spectra of achiral guests on the chiral silica. The achiral guests were: a) PhSiO_3 residues, b) porphyrin, and c) gold nanoparticles. d) Schematic illustration of geometrically ordered chiral blocks and achiral guests adsorbed on the silica walls.^[55] Copyright © 2012 WILEY-VCH Verlag GmbH & Co. KGaA, Weinheim.

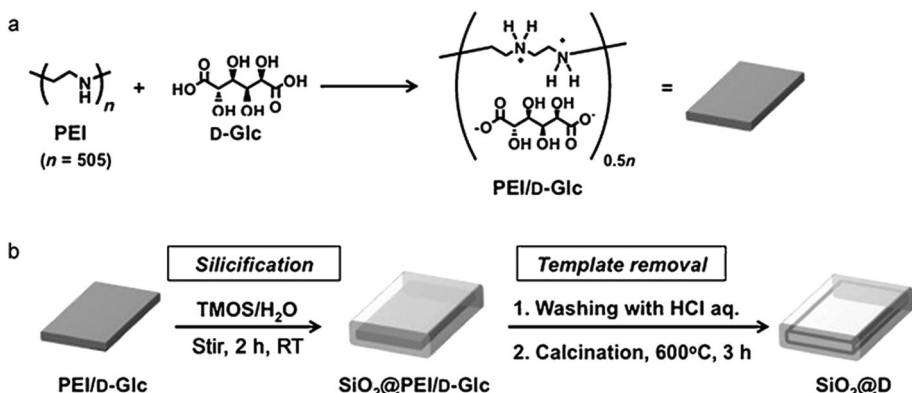


Figure 36. Illustration of chiral silica duplication from the complexation of α -glucaric acid (α -Glc) with linear PEI. a) Synthesis of supramolecular complexes consisting of PEI and α -Glc; b) preparation of silica replicas transcribed from PEI/ α -Glc complexes.^[56] Copyright © 2014 WILEY-VCH Verlag GmbH & Co. KGaA, Weinheim.

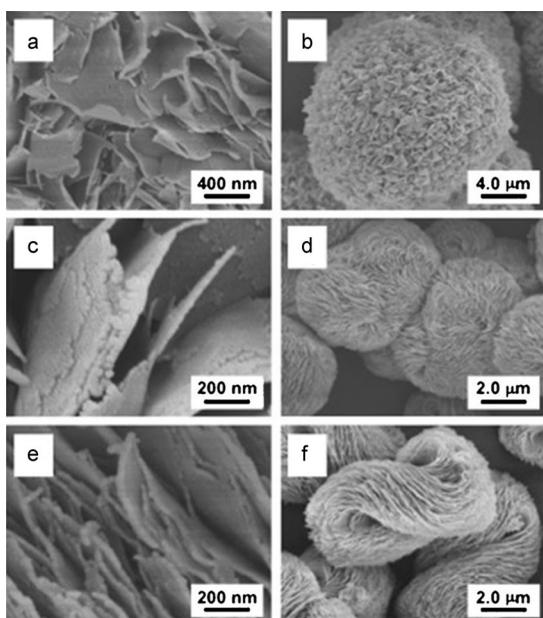


Figure 37. SEM images of Ca^{2+} -affected $\text{SiO}_2@\text{PEI}/\text{D-Glc-1}$ hybrids. PEI/ α -Glc complexes were prepared from PEI/ α -Glc solutions of different pH values: a), b) pH 4.53; c), d) pH 3.50; e), f) pH 3.00.^[56] Copyright © 2014 WILEY-VCH Verlag GmbH & Co. KGaA, Weinheim.

Summary and Outlook

This review mainly introduced the preparation of a series of silica nanomaterials with divergent morphologies and/or integrated chirality based on biomimetic mineralization techniques that use various polyamine/polypeptide-bearing templates under mild conditions and sol-gel reaction of chiral templates. Particularly, biosilica-inspired silicification employing the entities of self-assembled polyethylenimine via association with water or chiral acids show great potential in design and construction of integrated silica nanomaterials through a very simple route. As indicated by Müller et al. recently, the: "discovery of enzymatically driven biosilica synthesis opens a new avenue to fabricate patterned silica structures onto organic tem-

plates and by that this paradigm shift allows a major reorientation of methodology (traditional sol-to-gel polycondensation) allowing this old question to be approached in a new light (sol-to-gel biopolycondensation)".^[57]

Our PEI-based-biosilica-inspired approach is not limited in the design of silica materials. This has been extended to the preparation of other shaped functional inorganic nanomaterials, such as titania and rare-earth metal oxides. Of course, chiral metal oxides are also targeted in this extended program. The goal

of templating inorganic materials by organic molecules is not only to mimic nature, but also to program the morphology and chirality to advance the many applications dependent on their specific structures. Creation of chiral inorganic materials with biomimetic mineralization could provide new challenges for fusion of organic and inorganic components in the upgraded high level and for activation of their synergistic applications in many fields.

Acknowledgements

Portions of the research reviewed here were supported in part by Core Research for Evolutional Science and Technology (CREST), Japan Science and Technology Corporation (JST), by JSPS KAKENHI Grant-in-Aid for Scientific Research (B), no. 25288058 and by MEXT-Supported Program for the Strategic Research Foundation at Private Universities: "Creation of new fusion materials by integration of highly-ordered nano inorganic materials and ultra-precisely controlled organic polymers" (2013-2017).

Keywords: biomimetic silicification • chiral silica • nanostructured silica • self-assembly • sol-gel

- [1] J. Aizenberg, J. C. Weaver, M. S. Thanawala, V. C. Sundar, D. E. Morse, P. Fratzl, *Science* **2005**, *309*, 275–278.
- [2] S. S. Voznesenskiy, Y. N. Kul'chin, A. N. Galkina, *Nanotechnol. Russ.* **2011**, *6*, 43–78.
- [3] a) M. E. Davis, *Nature* **2002**, *417*, 813–821; b) D. Tarn, C. E. Ashley, M. Xue, E. C. Carnes, J. I. Zink, C. J. Brinker, *Acc. Chem. Res.* **2013**, *46*, 792–801; c) Y. D. Liu, J. Goebel, Y. D. Yin, *Chem. Soc. Rev.* **2013**, *42*, 2610–2653; d) K. Ariga, A. Vinu, Y. Yamauchi, Q. M. Ji, J. P. Hill, *Bull. Chem. Soc. Jpn.* **2012**, *85*, 1; e) K. Ariga, Q. M. Ji, T. Mori, M. Naito, Y. Yamauchi, H. Abe, J. P. Hill, *Chem. Soc. Rev.* **2013**, *42*, 6322–6345; f) J. Kopecek, J. Y. Yang, *Angew. Chem. Int. Ed.* **2012**, *51*, 7396–7417; *Angew. Chem.* **2012**, *124*, 7512–7535.
- [4] P. Tréguer, D. M. Nelson, A. J. van Bennekom, D. J. DeMaster, A. Leynaert, B. Quéguiner, *Science* **1995**, *268*, 375–379.
- [5] H. C. Schröder, X. Wang, W. Tremel, H. Ushijima, W. E. G. Müller, *Nat. Prod. Rep.* **2008**, *25*, 455–474.
- [6] M. Hildebrand, *Chem. Rev.* **2008**, *108*, 4855–4874.

- [7] F. E. Round, R. M. Crawford, D. G. Mann, *The Diatoms: Biology and Morphology of the Genera*, Cambridge University Press, 1990, pp. 1–10.
- [8] a) N. Kröger, C. Bergsdorf, M. Sumper, *Eur. J. Biochem.* **1996**, *239*, 259–284; b) N. Kröger, G. Lehmann, R. Rachel, M. Sumper, *Eur. J. Biochem.* **1997**, *250*, 99–105; c) N. Kröger, R. Deutzmann, M. Sumper, *Science* **1999**, *286*, 1129–1132; d) N. Kröger, R. Deutzmann, C. Bergsdorf, M. Sumper, *Proc. Natl. Acad. Sci. USA* **2000**, *97*, 14133–14138.
- [9] a) K. Shimizu, J. N. Cha, G. D. Stucky, D. E. Morse, *Proc. Natl. Acad. Sci. USA* **1998**, *95*, 6234–6238; b) J. N. Cha, K. Shimizu, Y. Zhou, S. C. Christensen, B. F. Chmelka, G. D. Stucky, D. E. Morse, *Proc. Natl. Acad. Sci. USA* **1999**, *96*, 361–365.
- [10] E. Dujardin, S. Mann, *Adv. Mater.* **2002**, *14*, 3392–3406.
- [11] C. Sanchez, H. Arribat, M. M. Giraud-Guilie, *Nat. Mater.* **2005**, *4*, 277–288.
- [12] a) R.-H. Jin, J.-J. Yuan, *Chem. Commun.* **2005**, 1399–1401; b) J.-J. Yuan, R.-H. Jin, *Langmuir* **2005**, *21*, 3136–3145; c) R.-H. Jin, J.-J. Yuan, *Macromol. Chem. Phys.* **2005**, *206*, 2160–2170; d) R.-H. Jin, J.-J. Yuan, *Chem. Mater.* **2006**, *18*, 3390–3396; e) H. Matsukizono, R.-H. Jin, *J. Nanopart. Res.* **2011**, *13*, 683–691; f) R.-H. Jin, J.-J. Yuan, *Polym.* **2007**, *39*, 822–827; g) P.-X. Zhu, R.-H. Jin, *Small* **2007**, *3*, 394–398; h) Matsukizono, P.-X. Zhu, N. Fukazawa, R.-H. Jin, *CrystEngComm* **2009**, *11*, 2695–2700; h) J.-J. Yuan, R.-H. Jin, *Langmuir* **2011**, *27*, 9588–9596; i) J.-J. Yuan, R.-H. Jin, *J. Mater. Chem.* **2011**, *21*, 10720–10729; j) R.-H. Jin, J.-J. Yuan, *Adv. Mater.* **2009**, *21*, 3750–3753; k) J.-J. Yuan, P.-X. Zhu, N. Fukazawa, R.-H. Jin, *Adv. Funct. Mater.* **2006**, *16*, 2205–2212; l) X.-L. Liu, P.-X. Zhu, Y.-F. Gao, R.-H. Jin, *Materials* **2012**, *5*, 1787–1799; m) X.-L. Liu, P.-X. Zhu, Y.-F. Gao, R.-H. Jin, *J. Mater. Chem. C* **2013**, *1*, 477–483; n) X.-L. Liu, Y.-F. Gao, R.-H. Jin, H. Luo, P. Peng, Y. Liu, *Nano Energy* **2014**, *4*, 31–38; o) R.-H. Jin, J.-J. Yuan, *Advances in Biomimetics*, 2011, DOI: 10.5772/14905.
- [13] a) J. J. Yuan, O. O. Mykhaylyk, A. J. Ryan, S. P. Armes, *J. Am. Chem. Soc.* **2007**, *129*, 1717–1723; b) J. Z. Du, S. P. Armes, *Langmuir* **2009**, *25*, 9564–9570; c) J. Z. Du, S. P. Armes, *Langmuir* **2008**, *24*, 13710–13716; d) Y. Y. Li, J. Z. Du, S. P. Armes, *Macromol. Rapid Commun.* **2009**, *30*, 464–468.
- [14] A. Khanal, Y. Inoue, M. Yada, K. Nakashima, *J. Am. Chem. Soc.* **2007**, *129*, 1534–1535.
- [15] C. L. Wu, X. Wang, L. Z. Zhao, Y. H. Gao, R. J. Ma, Y. L. An, L. Q. Shi, *Langmuir* **2010**, *26*, 18503–18507.
- [16] B. Y. Du, Z. Cao, Z. B. Li, A. X. Mei, X. H. Zhang, J. J. Nie, J. T. Xu, Z. Q. Fan, *Langmuir* **2009**, *25*, 12367–12373.
- [17] M. W. Pi, T. T. Yang, J. J. Yuan, S. Fujii, Y. Kakigi, Y. Nakamura, S. Y. Cheng, *Colloids Surf. B: Biointerfaces* **2010**, *78*, 193–199.
- [18] H. Q. Li, C. S. Ha, I. Kim, *Langmuir* **2008**, *24*, 10552–10556.
- [19] a) M. Müllner, T. Lunkenstein, J. Breu, F. Caruso, A. H. E. Müller, *Chem. Mater.* **2012**, *24*, 1802–1810; b) J. Y. Yuan, Y. Y. Xu, A. Walther, S. Bolisetty, M. Schumacher, H. Schmalz, M. Ballauff, A. H. E. Müller, *Nat. Mater.* **2008**, *7*, 718–722; c) M. Müllner, J. Y. Yuan, S. Weiss, A. Walther, M. Förtsch, M. Drechsler, A. H. E. Müller, *J. Am. Chem. Soc.* **2010**, *132*, 16587–16592.
- [20] a) K. Zhang, L. Gao, Y. M. Chen, *Macromolecules* **2007**, *40*, 5916–5922; b) K. Zhang, L. Gao, Y. M. Chen, *Macromolecules* **2008**, *41*, 1800–1807; c) Y. M. Chen, *Macromolecules* **2012**, *45*, 2619–2631; d) D. D. Yao, Y. J. Guo, S. G. Chen, J. N. Tang, Y. M. Chen, *Polymer* **2013**, *54*, 3485–3491; e) J. L. Qin, Y. M. Chen, *Acta Polym. Sin.* **2011**, *6*, 572–585.
- [21] a) L. Xia, Z. B. Li, *Langmuir* **2011**, *27*, 1116–1122; b) H. Chen, L. Xia, W. X. Fu, Z. Y. Yang, Z. B. Li, *Chem. Commun.* **2013**, *49*, 1300–1302; c) L. Xia, Y. Liu, Z. B. Li, *Macromol. Biosci.* **2010**, *10*, 1566–1575.
- [22] J. E. Meegan, A. Aggeli, N. Boden, R. Brydson, A. P. Brown, L. Carrick, A. R. Brough, A. Hussain, R. J. Ansell, *Adv. Funct. Mater.* **2004**, *14*, 31–37.
- [23] S. C. Holmström, P. J. S. King, M. G. Ryadnov, M. F. Butler, S. Mann, D. N. Woolfson, *Langmuir* **2008**, *24*, 11778–11783.
- [24] S. J. Wang, X. Ge, J. Y. Xue, H. M. Fan, L. J. Mu, Y. P. Li, H. Xu, J. R. Lu, *Chem. Mater.* **2011**, *23*, 2466–2474.
- [25] V. M. Yuwono, J. D. Hartgerink, *Langmuir* **2007**, *23*, 5033–5038.
- [26] E. Kasotakis, A. Mitraki, *Biopolymers* **2012**, *97*–*98*, 501–509.
- [27] A. Altunbas, N. Sharma, M. S. Lamm, C. Q. Yan, R. P. Nagarkar, J. P. Schneider, D. J. Pochan, *ACS Nano* **2010**, *4*, 181–188.
- [28] K. M. Hawkins, S. S. S. Wang, D. M. Ford, D. F. Shantz, *J. Am. Chem. Soc.* **2004**, *126*, 9112–9119.
- [29] A. Gabashvili, D. D. Medina, A. Gedanken, Y. Mastai, *J. Phys. Chem. B* **2007**, *111*, 11105–11110.
- [30] a) P. T. Tanev, Y. Liang, T. J. Pinnavaia, *J. Am. Chem. Soc.* **1997**, *119*, 8616–8624; b) S. S. Kim, W. Zhang, T. J. Pinnavaia, *Science* **1998**, *282*, 1302–1305.
- [31] K. Katagiri, K. Ariga, J. Kikuchi, *Chem. Lett.* **1999**, 661–662; d) Y. Lu, H. Fan, A. Stump, T. L. Ward, T. Rieker, C. J. Brinker, *Nature* **1999**, *398*, 223–226.
- [32] a) D. H. W. Hubert, M. Jung, P. M. Frederick, P. H. H. Bomans, J. Meuldijk, A. L. German, *Adv. Mater.* **2000**, *12*, 1286–1290; b) D. H. W. Hubert, M. Jung, A. L. German, *Adv. Mater.* **2000**, *12*, 1291–1294.
- [33] H. P. Lin, Y. R. Cheng, C. Y. Mou, *Chem. Mater.* **1998**, *10*, 3772–3776.
- [34] a) S. Baral, P. Schoen, *Chem. Mater.* **1993**, *5*, 145–147.
- [35] D. D. Archibald, S. Mann, *Nature* **1993**, *364*, 430–433.
- [36] a) M. Adachi, T. Harada, M. Harada, *Langmuir* **1999**, *15*, 7097–7100; b) M. Adachi, T. Harada, M. Harada, *Langmuir* **2000**, *16*, 2376–2384; c) M. Harada, M. Adachi, *Adv. Mater.* **2000**, *12*, 839–841.
- [37] J. S. Beck, J. C. Vartuli, W. J. Roth, M. E. Leonowicz, C. T. Kresge, K. D. Schmitt, C. T.-W. Chu, D. H. Olson, E. W. Sheppard, S. B. McCullen, J. B. Higgins, J. L. Schlenker, *J. Am. Chem. Soc.* **1992**, *114*, 10834–10843.
- [38] J. H. Jung, M. Amaike, S. Shinkai, *Chem. Commun.* **2000**, 2343–2344.
- [39] D. Eglin, G. Mosser, M. M. Giraud-Guilie, J. Livage, T. Coradin, *Soft Matter* **2005**, *1*, 129–131.
- [40] R. L. Brutney, D. E. Morse, *Chem. Rev.* **2008**, *108*, 4915–4934.
- [41] J. H. Jung, Y. Ono, S. Shinkai, *Chem. Eur. J.* **2000**, *6*, 4552–4557.
- [42] J. H. Jung, H. Kobayashi, M. Masuda, T. Shimizu, T. Shinkai, *J. Am. Chem. Soc.* **2001**, *123*, 8785–8789.
- [43] a) J. H. Jung, K. Yoshida, T. Shimizu, *Langmuir* **2002**, *18*, 8724–8727; b) J. H. Jung, S. Shinkai, T. Shimizu, *Chem. Rec.* **2003**, *3*, 212–224.
- [44] K. Sugiyasu, S. Tamaru, M. Takeuchi, D. Berthier, I. Huc, R. Oda, S. Shinkai, *Chem. Commun.* **2002**, 1212–1213.
- [45] T. Delclos, C. Aimé, E. Pouget, A. Brizard, I. Huc, M.-H. Delville, R. Oda, *Nano Lett.* **2008**, *8*, 1929–1935.
- [46] a) Y. Y. Lin, Y. Qiao, C. Gao, P. F. Tang, Y. Liu, Z. B. Li, Y. Yan, J. B. Huang, *Chem. Mater.* **2010**, *22*, 6711–6717; b) Y. Yan, Y. Y. Lin, Y. Qiao, J. B. Huang, *Soft Matter* **2011**, *7*, 6385–6398.
- [47] S. Che, Z. Liu, T. Ohsuna, K. Sakamoto, O. Tersarki, T. Tatsumi, *Nature* **2004**, *429*, 281–284.
- [48] H. Jin, Z. Liu, T. Ohsuna, O. Terasaki, Y. Inoue, K. Sakamoto, T. Nakanishi, K. Ariga, S. Che, *Adv. Mater.* **2006**, *18*, 593–596.
- [49] J. Wang, W. Wang, P. Sun, Z. Yuan, B. Li, Q. Jin, D. Ding, T. Chen, *J. Mater. Chem.* **2006**, *16*, 4117–4122.
- [50] a) H. Yang, G. A. Ozin, C. T. Kresge, *Adv. Mater.* **1998**, *10*, 883–887; b) M. Antonietti, G. A. Ozin, *Chem. Eur. J.* **2004**, *10*, 28–41.
- [51] Y. Li, L. Bi, S. Wang, Y. Chen, B. Li, X. Zhu, Y. Yang, *Chem. Commun.* **2010**, *46*, 2680–2682.
- [52] B. Li, Y. Chen, H. Zhao, X. Pei, L. Bi, K. Hanabusa, Y. Yang, *Chem. Commun.* **2008**, 6366–6368.
- [53] Y. Li, B. Li, Z. Yan, Z. Xiao, Z. Huang, K. Hu, S. Wang, Y. Yang, *Chem. Mater.* **2013**, *25*, 307–312.
- [54] a) Y. Snir, R. D. Kamien, *Science* **2005**, *307*, 1067; b) Y. Han, L. Zhao, J. Y. Ying, *Adv. Mater.* **2007**, *19*, 2454–2459.
- [55] H. Matsumoto, R.-H. Jin, *Angew. Chem. Int. Ed.* **2012**, *51*, 5862–5865; *Angew. Chem.* **2012**, *124*, 5964–5967.
- [56] H. Matsumoto, H. Murata, R.-H. Jin, *Chem. Eur. J.* **2014**, *20*, 1134–1145.
- [57] W. E. G. Müller, H. C. Schroder, Z. Burghard, D. Pisignano, X. Wang, *Chem. Eur. J.* **2013**, *19*, 5790–5804.

Published online on May 26, 2014